

# UC Davis

## UC Davis Previously Published Works

### Title

Hydrodynamics structure plankton communities and interactions in a freshwater tidal estuary

### Permalink

<https://escholarship.org/uc/item/5d66x81p>

### Journal

Ecological Monographs, 93(2)

### ISSN

0012-9615

### Authors

Smits, Adrienne P  
Loken, Luke C  
Van Nieuwenhuysse, Erwin E  
et al.

### Publication Date

2023-05-01






### DOI

10.1002/ecm.1567

Peer reviewed

## ARTICLE

# Hydrodynamics structure plankton communities and interactions in a freshwater tidal estuary

Adrienne P. Smits<sup>1</sup>  | Luke C. Loken<sup>1,2</sup>  | Erwin E. Van Nieuwenhuysen<sup>3</sup> |  
 Matthew J. Young<sup>4</sup>  | Paul R. Stumpner<sup>5</sup> | Leah E. K. Lench<sup>5</sup>  |  
 Jon R. Burau<sup>5</sup> | Randy A. Dahlgren<sup>6</sup> | Tiffany Brown<sup>7</sup> | Steven Sadro<sup>1</sup> 

<sup>1</sup>Department of Environmental Science and Policy, University of California Davis, Davis, California, USA

<sup>2</sup>United States Geological Survey, Upper Midwest Water Science Center, Madison, Wisconsin, USA

<sup>3</sup>Bureau of Reclamation, Science Division, Bay-Delta Office, Sacramento, California, USA

<sup>4</sup>US Geological Survey, California Water Science Center, Sacramento, California, USA

<sup>5</sup>US Geological Survey, California Water Science Center, West Sacramento, California, USA

<sup>6</sup>Department of Land, Air, and Water Resources, University of California Davis, Davis, California, USA

<sup>7</sup>California Department of Water Resources, West Sacramento, California, USA

**Correspondence**

Adrienne P. Smits  
 Email: [asmits@ucdavis.edu](mailto:asmits@ucdavis.edu)

**Funding information**

Bureau of Reclamation, Grant/Award Numbers: R18AC00040, R20PG00028

**Handling Editor:** Stuart E. Jones

**Abstract**

Drivers of phytoplankton and zooplankton dynamics vary spatially and temporally in estuaries due to variation in hydrodynamic exchange and residence time, complicating efforts to understand controls on food web productivity. We conducted approximately monthly (2012–2019;  $n = 74$ ) longitudinal sampling at 10 fixed stations along a freshwater tidal terminal channel in the San Francisco Estuary, California, characterized by seaward to landward gradients in water residence time, turbidity, nutrient concentrations, and plankton community composition. We used multivariate autoregressive state space (MARSS) models to quantify environmental (abiotic) and biotic controls on phytoplankton and mesozooplankton biomass. The importance of specific abiotic drivers (e.g., water temperature, turbidity, nutrients) and trophic interactions differed significantly among hydrodynamic exchange zones with different mean residence times. Abiotic drivers explained more variation in phytoplankton and zooplankton dynamics than a model including only trophic interactions, but individual phytoplankton–zooplankton interactions explained more variation than individual abiotic drivers. Interactions between zooplankton and phytoplankton were strongest in landward reaches with the longest residence times and the highest zooplankton biomass. Interactions between cryptophytes and both copepods and cladocerans were stronger than interactions between bacillariophytes (diatoms) and zooplankton taxa, despite contributing less biovolume in all but the most landward reaches. Our results demonstrate that trophic interactions and their relative strengths vary in a hydrodynamic context, contributing to food web heterogeneity within estuaries at spatial scales smaller than the freshwater to marine transition.

**KEYWORDS**

estuary, food web, hydrodynamics, phytoplankton, San Francisco estuary, time series, trophic interactions, zooplankton

This is an open access article under the terms of the [Creative Commons Attribution](https://creativecommons.org/licenses/by/4.0/) License, which permits use, distribution and reproduction in any medium, provided the original work is properly cited.

© 2023 The Authors. *Ecological Monographs* published by Wiley Periodicals LLC on behalf of The Ecological Society of America.

## INTRODUCTION

Estuaries are among the most productive aquatic ecosystems (Hoellein et al., 2013; Winder et al., 2017). However, hydrologic alterations, land conversion, agricultural and urban pollution, fisheries exploitation, species invasions, and climate warming have severely impacted many of the world's estuaries (Kennish, 2002), with negative consequences for food web productivity and biodiversity (Lotze et al., 2006). In some highly impacted estuaries, phytoplankton production has increased to detrimental levels that promote hypoxia or anoxia (Howarth et al., 2011), or has shifted toward non-nutritious or harmful species (Paerl et al., 2010). In others, phytoplankton productivity has decreased (e.g., the San Francisco Estuary; Jassby et al., 2002; Kimmerer et al., 2012), causing changes to food web structure and declines in zooplankton and pelagic fishes (Sommer et al., 2007; Winder & Jassby, 2011). Anthropogenic stressors tend to occur simultaneously and affect both “bottom-up” and “top-down” processes (Lotze & Milewski, 2004), complicating efforts to understand changes to pelagic food webs in estuaries.

Drivers of phytoplankton and zooplankton productivity and biomass are inherently difficult to quantify in estuaries, where inter-annual and seasonal variability in environmental conditions overlay spring-neap and daily variation caused by tidal hydrodynamics. Interactions among tidal forces, morphology, and freshwater inputs generate spatial variation in water exchange rates and the distribution of dissolved and suspended constituents, including phytoplankton and zooplankton. For example, estuarine turbidity maxima created by density-driven currents are often sites of chlorophyll *a* accumulation and high zooplankton productivity, despite light-limitation of in situ primary production (Lapierre & Frenette, 2008; Lee et al., 2012). In estuarine terminal channels and sloughs, variation in tidal forcing and tidal excursion length creates distinct hydrodynamic zones with different water exchange rates (Stumpner, Burau, & Forrest, 2020), while tidal asymmetry produces variation in turbidity (e.g., light availability) and nutrient concentrations (Feyrer et al., 2017; Loken et al., 2022), all of which can potentially influence phytoplankton productivity.

In addition to affecting primary production rates, spatio-temporal variation in hydrodynamics, inflows, and residence time (i.e., how long a water parcel remains within a water body before exiting; Monsen et al., 2002) structure phytoplankton and zooplankton community composition (Suzuki et al., 2013; Valdes-Weaver et al., 2006), and control biomass accumulation in estuaries and rivers (Bum & Pick, 1996; Pace et al., 1992). For example, the Upper Mississippi River exhibits lateral differences in phytoplankton biomass and community composition

between main channels and backwaters related to residence time and associated factors (e.g., turbidity; Manier et al., 2021; Jankowski et al., 2021). In the Frazier River estuary, short residence times caused by spring snowmelt discharge and exacerbated by channelization reduced zooplankton biomass and altered species composition relative to adjacent slough habitats (Breckenridge et al., 2015). Such variation in the community composition of producers and consumers can influence the trophic efficiency of pelagic food webs (Dickman et al., 2008) and food quality for predators such as fishes (Winder & Jassby, 2011).

Though many estuaries are considered primarily “bottom-up” systems, in which phytoplankton biomass is limited by abiotic controls on primary production (Cloern, 1987), some estuaries or estuarine habitats exhibit top-down control on phytoplankton biomass (e.g., control by grazing; Tan et al., 2004; Thompson et al., 2008; Wetz et al., 2011). Phytoplankton dynamics respond to combinations of abiotic and biotic drivers, with the relative importance of each changing spatially and across seasons (Guinder et al., 2017). Trophic linkages between phytoplankton and zooplankton are stronger in long-residence time estuarine habitats, such as terminal channels, than in more dynamic environments (Young, Feyrer, et al., 2021). However, we still lack a complete understanding of how hydrodynamic complexity dictates the relative importance of abiotic and biotic controls on pelagic food webs in estuaries.

Bottom-up and top-down drivers of phytoplankton and zooplankton dynamics vary spatially within estuaries and other aquatic systems; therefore, approaches accounting for spatial variation are necessary to understand food web processes. Though long-term trends and inter-annual variation in phytoplankton and zooplankton community composition and biomass have been related to discrete disturbances such as species introductions or hydrologic extremes (Dexter et al., 2020; Harding et al., 2016; Kratina et al., 2014), spatially distributed time series with the temporal resolution and length to capture seasonal and inter-annual variation, as well as the taxonomic resolution to quantify trophic interactions, remain rare in estuarine ecosystems, though they are commonly collected by lake monitoring programs (Hampton et al., 2019). Time series modeling has been successfully applied in freshwater and marine ecosystems to quantify abiotic and biotic controls on food web dynamics at bi-weekly to monthly time scales (Dexter et al., 2020; Griffiths et al., 2016; Hampton et al., 2006; Walsh et al., 2018), but to our knowledge this approach has not yet been used in estuaries.

Our goal was to characterize how hydrodynamic processes (e.g., water exchange) mediates drivers of temporal variation in phytoplankton and zooplankton

biomass in the northern Sacramento-San Joaquin River Delta (hereafter, the “Delta”), a freshwater tidal portion of the San Francisco Estuary (SFE). Understanding these dynamics in the SFE is necessary to quantify food availability for threatened native fishes such as the Delta Smelt (*Hypomesus transpacificus*), the health and fitness of which are positively correlated with chlorophyll *a* and zooplankton biomass (Hammock et al., 2021). We conducted longitudinal sampling along a terminal

channel in the north Delta (Figure 1), characterized by spatial gradients in water residence time (Downing et al., 2016; Stumpner, Burau, & Forrest, 2020), turbidity (Feyrer et al., 2017), and nutrient concentrations (Loken et al., 2022). The morphological simplicity and stable spatial gradients present within the study channel allowed us to test for the effects of water exchange and residence time on drivers of plankton biomass.

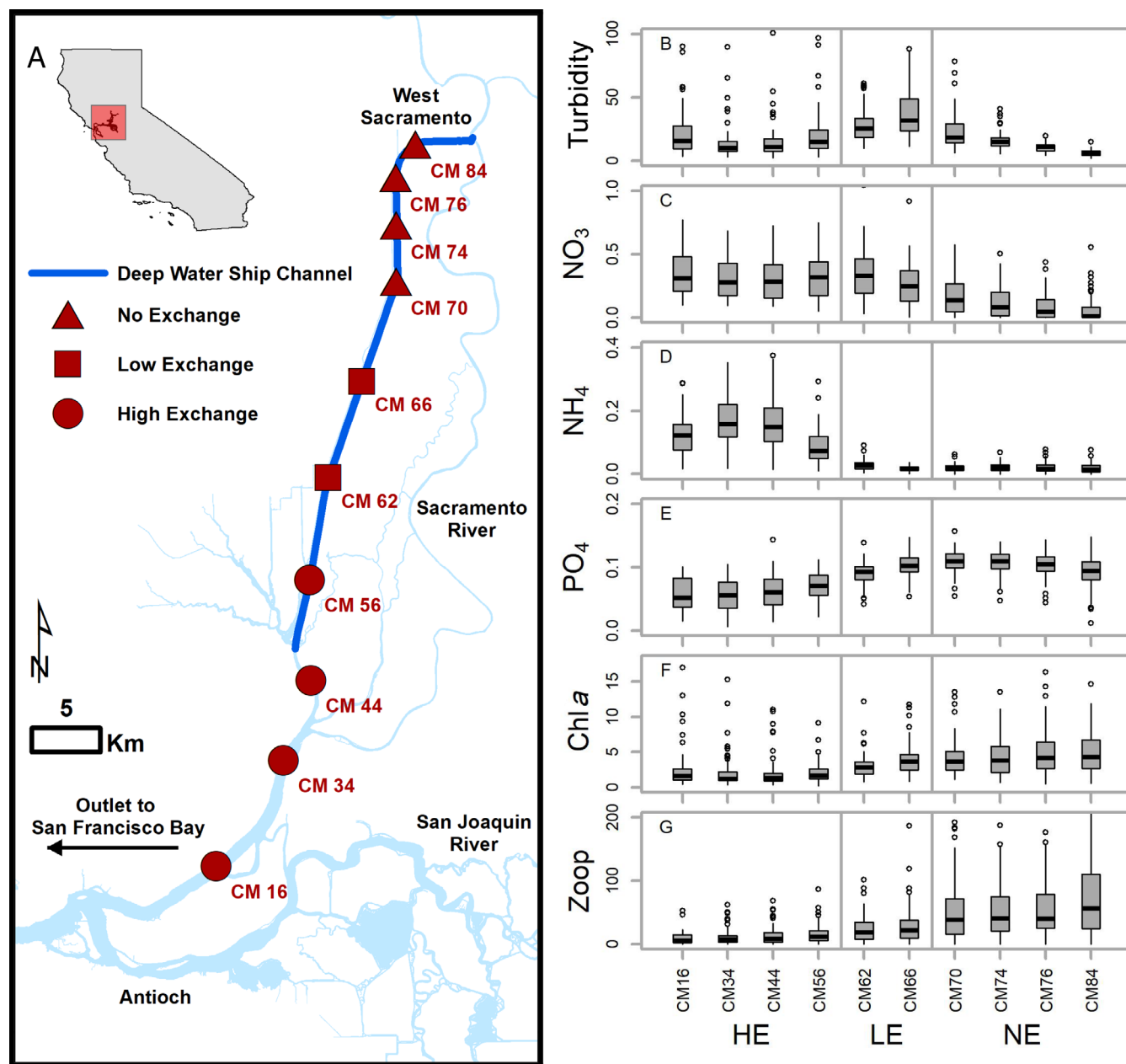


**FIGURE 1** (A) Location of sampling stations (designated by channel markers; CM) within each hydrodynamic exchange zone (HE, high exchange; LE, low exchange; NE, no exchange). (B–G) Turbidity (Nephelometric Turbidity Units [NTU]), nitrate concentration (mg N L<sup>-1</sup>), ammonium (mg N L<sup>-1</sup>), phosphate (mg P L<sup>-1</sup>), chlorophyll *a* (μg L<sup>-1</sup>), and total zooplankton biomass (μg dw L<sup>-1</sup>) at each sampling station, including all sampling dates (2012–2019). Sampling stations on the x-axes are ordered from seaward to landward (CM 16–84), and gray vertical lines denote site groupings based on hydrodynamic exchange zones.

We asked three questions: (1) Do environmental drivers of phytoplankton and (2) zooplankton biomass vary along a spatial gradient in water exchange and water residence time? and (3) Do trophic interactions between zooplankton and phytoplankton vary across these gradients? We used multivariate autoregressive state space (MARSS; Holmes et al., 2012) models to investigate phytoplankton and zooplankton dynamics at a monthly time scale and to explicitly test for spatial variation in drivers and trophic interactions.

## METHODS

### Study system

We conducted our study in the northern Delta, a freshwater tidal portion of the SFE, a large and highly altered estuary on the Pacific coast of North America. Widespread conversion of wetlands to agricultural production, water diversions, and channel alterations, and successive species invasions have resulted in dramatic declines in phytoplankton productivity and pelagic organism biomass throughout the SFE and Delta (Sommer et al., 2007). Historically, the Delta contained extensive tidal wetlands and terminal sloughs, most of which have been converted to agricultural land or rock-hardened channels (Whipple et al., 2012). The few remaining shallow water habitats sustain relatively high phytoplankton and zooplankton densities relative to the greater Delta (Montgomery et al., 2017; Stumpner, Bergamaschi, et al., 2020), as well as small populations of endangered native fishes (Sommer & Mejia, 2013).

Our study sites were located in a terminal channel formed by the upper portions of the Sacramento River Deep Water Ship Channel (DWSC; Figure 1A), which connects the West Sacramento Port to the Sacramento River and San Francisco Bay/Pacific Ocean. The 69 km long channel has a width of ~150 m, depth of ~10 m, and has one set of non-operational ships locks at its northern terminus. The channel is tidally forced and functionally resembles a large, morphologically homogenous dead-end slough with minimal net flow (Feyrer et al., 2017).

We sampled at 10 fixed sites along the DWSC, identified by channel marker (CM) number, to characterize water quality parameters and plankton community composition and biomass (Figure 1; depths 9.8–12.8 m). Study sites were located in three distinct hydrodynamic zones: the no-exchange zone (NE), where waters are trapped in the upper, landward section of the DWSC (above CM 70); a zone of mixing and high turbidity in the mid-zone (CM62–CM66; low-exchange = LE); and the seaward zone that experiences tidal exchange each

day (below CM62; high exchange zone = HE; Stumpner, Burau, & Forrest, 2020). These contrasting hydrodynamic conditions create a strong gradient in water residence time, water quality, and food resources across sites (Stumpner, Burau, & Forrest, 2020; Young, Feyrer, et al., 2021). Water residence time is ~1 day in the HE zone, >7 days in the LE zone, and several weeks to months in the NE zone (Stumpner, Burau, & Forrest, 2020).

### Sample collection and processing

We collected water chemistry and plankton samples at each station approximately monthly from April 2012 until September 2019 (74 sampling dates). Two YSI 6600 probes were used to collect field measurements of temperature and specific conductance. Turbidity was measured in the field on samples collected from 1 m depth using a Hach 2100P turbidimeter.

Two 1-L water chemistry samples were collected at 1 m depth using a submerged water pumping system and stored in acid-washed HDPE bottles for laboratory analyses. A 500 mL water sample for phytoplankton identification and biovolume quantification was collected at 1-m depth and preserved in 3% Lugol's solution (final concentration). Zooplankton samples were collected by vertical tow using a 150- $\mu\text{m}$  mesh zooplankton net with a retrieval rate of  $\sim 0.33 \text{ m s}^{-1}$ . The 150- $\mu\text{m}$  mesh size was selected to avoid complications from high suspended sediment concentrations that frequently occur at some sampling sites, but as a result, smaller life stages (nauplii, early copepodites) and microzooplankton were not sampled effectively (Kayfetz et al., 2020). Zooplankton samples were preserved in a 2% final concentration of Lugol's solution.

Sample processing was initiated within 24 h of collection time. A subsample was filtered through a pre-rinsed 0.2  $\mu\text{m}$  polycarbonate membrane (Millipore) for quantification of soluble reactive phosphorus (SR- $\text{PO}_4$ ), nitrate-N ( $\text{NO}_3\text{-N}$ ) + nitrite-N ( $\text{NO}_2\text{-N}$ ), and ammonium ( $\text{NH}_4\text{-N}$ ). SR- $\text{PO}_4$  was determined using the ammonium molybdate spectrophotometric method (limit of detection (LOD)  $\sim 0.005 \text{ mg L}^{-1}$ ; Clesceri et al., 1998). The vanadium chloride method was used to spectroscopically determine  $\text{NO}_3 + \text{NO}_2\text{-N}$  (LOD =  $0.01 \text{ mg L}^{-1}$ ; Doane & Horwath, 2003). As  $\text{NO}_3\text{-N}$  constituted >95% of the combined  $\text{NO}_3 + \text{NO}_2\text{-N}$  concentration, we report the  $\text{NO}_3 + \text{NO}_2\text{-N}$  concentration as  $\text{NO}_3\text{-N}$  in this study.  $\text{NH}_4\text{-N}$  was determined spectroscopically with the Berthelot reaction, using a salicylate analog of indophenol blue (LOD  $\sim 0.010 \text{ mg L}^{-1}$ ; Forster, 1995). Dissolved Si was determined using the molybdate-reactive spectroscopic method (SM4500-SiO<sub>2</sub> C; MRL =  $0.5 \text{ mg L}^{-1}$ ; Clesceri et al., 1998).

Chlorophyll *a* concentrations were determined from duplicate samples collected on Whatman GF/F filters, following methods in Clesceri et al. (1998). Samples were filtered in the field using low vacuum and stored on ice until storage in a  $-20^{\circ}\text{C}$  freezer. Samples were extracted in 90% ethanol, and filters were freeze dried but not ground (Sartory & Grobbelaar, 1984). Samples were analyzed by fluorometric determination with the limit of detection dependent on the volume of water filtered (200–1000 mL, generally  $0.5\ \mu\text{g L}^{-1}$ ).

Phytoplankton identification and enumeration were performed using standard membrane filtration (McNabb, 1960). A Leica DMLB compound microscope was used for random field counts of at least 300 natural units and taxa were identified to the lowest possible taxonomic level. Cell biovolumes were quantified on a per milliliter basis (Hillebrand et al., 1999). In order to assess spatial and temporal variation in food quality for mesozooplankton, cyanobacteria or other taxa capable of producing toxins, for example, *Microcystis*, *Anabaena*, *Planktothrix*, *Peridinium*, and long-filament-forming taxa such as *Melosira* and *Aulacoseira*, were classified as “low” quality (Galloway & Winder, 2015; Jungbluth et al., 2021). All other phytoplankton taxa were classified as “high” quality.

Zooplankton abundance and identification were measured on three 1-mL aliquots using a Wilovert inverted microscope at  $100\times$  with a target tally of 200–400 specimens. Biomass estimates were based on established length/width relationships (Dumont et al., 1975; Lawrence et al., 1987; McCauley, 1984).

On five dates between June 2012 and October 2015, we collected samples for water isotopes ( $\delta^{18}\text{O}\text{-H}_2\text{O}$  and  $\delta^2\text{H}\text{-H}_2\text{O}$ ) at each station to characterize spatial patterns in water residence time (Downing et al., 2016). Samples were collected into 2-mL glass vials, overfilled for  $\sim 15\ \text{s}$  using a peristaltic pump, and capped without headspace. Vials for  $\delta^{18}\text{O}\text{-H}_2\text{O}$  and  $\delta^2\text{H}\text{-H}_2\text{O}$  were analyzed at the Stable Isotope Facility at the University of California-Davis using a laser water isotope analyzer. Stable isotopic composition of oxygen and hydrogen are reported in the text using delta ( $\delta$ ) notation,

$$\delta^{18}\text{O} \text{ or } \delta^2\text{H} (\text{‰}) = \left( \left( \frac{R_{\text{sample}}}{R_{\text{standard}}} \right) - 1 \right) \times 1000, \quad (1)$$

where  $R_{\text{sample}}$  and  $R_{\text{standard}}$  are ratios of heavy to light isotopes ( $^{18}\text{O}:^{16}\text{O}$  or  $^2\text{H}:^1\text{H}$ ) in samples and Vienna Standard Mean Ocean Water (VSMOW), respectively. Analytical precision was  $\pm 0.2\text{‰}$  for  $\delta^{18}\text{O}$  and  $\pm 1\text{‰}$  for  $\delta^2\text{H}$ . A more enriched (less negative) value indicates longer water residence time (greater water age) and more evaporation.

## Quantifying hydrodynamic conditions

Since hydrodynamic processes can affect constituents over short (hours to days) to long (weeks–months) timescales we used several metrics that vary over longer timescales to more closely align with the time scale (monthly) of sample collection. Tidally averaged discharge (hourly; cubic feet per second) was obtained from two United States Geological Survey (USGS) monitoring stations, one near Cache Slough in the HE zone (CM 45, USGS 11455350) and one within the DWSC (CM 54; USGS 11455335; US Geological Survey, 2021). Tidally-averaged discharge at CM 45 was used as a metric of seasonal hydrology for sites in the HE zone—when high flow events through the Yolo Bypass were excluded, it was highly correlated ( $R = 0.81$ ) with Sacramento River discharge at Freeport (USGS 11447650). In the landward LE and NE zones, we used discharge at CM 54 to capture variation in flow conditions (no gauges exist within the NE zone).

Normalized tidal amplitude was computed as a measure of tidal strength that varies from spring-neap ( $\sim 14$  days) to yearly timescales. During periods of higher tidal amplitude (normalized values greater than 1) water parcels are subject to stronger mixing and longer transport, decreasing water residence time. During periods of lower tidal amplitude (normalized values less than 1) water parcels will have less transport and mixing, with commensurately longer water residence time. Normalized tidal amplitude was estimated for each discrete sampling event. Discharge (15 min frequency) at CM 45 and CM 54 was used for the normalized tidal amplitude calculation. Because the discharge time series at CM45 ended prior to the end of the study, we substituted discharge at CM 41 (USGS 11455385) for the four missing dates (May–August 2019). For each discharge signal ( $Q$ ) the tidally filtered discharge ( $\langle Q \rangle$ ) was computed using a Godin filter (Godin, 1972), and the tidal discharge ( $Q'$ ) was computed as  $Q' = Q - \langle Q \rangle$ . The  $Q'$  signal was then used to compute the tidal amplitude by finding the outer envelopes (or tidal maxima) using a 30-h. moving window. The tidal amplitude is the difference between the upper and lower envelope, which was then normalized by median tidal amplitude over the length of the record.

We used tidal excursion length to assign fixed sampling stations to each of the three hydrodynamic zones (HE, LE, or NE) on each sampling date, and designated final site groupings based on a combination of hydrodynamic and environmental characteristics. Exchange zones were defined based on estimates of tidal excursion from the mouth of the DWSC using methods developed in Stumpner, Burau, and Forrest (2020) and Young, Feyrer, et al. (2021), and are a proxy for water residence time. The tidal excursion from the mouth of the DWSC

was estimated using water velocity data at CM 54, which was then corrected by a scaling factor of 1.54 based on comparison to drifters that traveled up the channel over a course of a single flood tide. Corrected water velocity was then integrated over each tidal period (~25 h) continuously over the length of the record to provide an estimate of the distance traveled along the DWSC. The distance traveled along the channel defines the upper boundary of the HE zone. The range of tidal excursions, over a month, was used to bound the LE zone. As a result, the boundaries of the HE and LE zones varied based on the tides, and the boundary of the LE zone also varied on monthly timescales due to the variation in the range of tidal excursions across spring-neap cycles.

For stations that switched zones between sampling dates (CM 56, CM 62), group assignment was based on both the proportion of sampling dates the site fell within each zone, as well as by comparing average water quality parameters with nearby stations. CM 56 fell within the HE zone on 57% of sampling dates, within the LE zone on 39% of sampling dates, and the NE zone on 4% of dates, and it was therefore grouped with stations in the HE zone. CM 62 fell within the LE zone on 39% of sampling dates and within the NE on 56% of sampling dates, but was assigned to the LE group based on its high mean turbidity. Although CM 66 technically fell within the NE zone, we assigned it to the LE zone based on its high turbidity.

## Seasonal phenology

We assessed seasonal trends in environmental variables and plankton biomass in each hydrodynamic zone by fitting generalized additive mixed models (GAMM's) to the data, using the “mgcv” package in R (Wood, 2022). We fitted each variable to month of year (1–12) using cyclic cubic regression smoothers, and we assessed spatial (i.e., among-zone) differences in seasonality by including a random effect of hydrodynamic zone for the seasonal trend.

## Time series analysis

For use in times series models, species-level phytoplankton biovolume ( $\mu\text{m}^3 \text{L}^{-1}$ ) or mesozooplankton biomass ( $\mu\text{g}$  dry weight  $\text{L}^{-1}$ ) were summed according to the following taxonomic divisions, which represent the dominant taxa in our study system: Bacillariophyta, Chlorophyta, and Cryptophyta (phytoplankton; Appendix S1: Figure S1), and Copepoda and Cladocera (zooplankton; Appendix S1: Figure S2). Phytoplankton

and zooplankton time series were aggregated by month. We used mean values for months with multiple sampling events. Monthly biovolume or biomass data were log-transformed. For taxa with zero biovolume or biomass at a given site and month, zeroes were replaced with  $\frac{1}{2}$  the lowest value prior to log-transformation. Chlorophytes had zero biovolume in 12% of 880 total sampling events (sites  $\times$  dates), cryptophytes in 1%, and cladocerans in 6%.

Environmental variables that were included as covariates (predictors) in time series models were aggregated to monthly values, as for plankton data. In addition to variables measured at each station during discrete sampling events, we used tidally-averaged discharge and normalized tidal amplitude at CM 45 (for stations within the HE zone) and CM 54 (stations within the LE and NE zones) to characterize temporal variation in flow and tidal strength. For these two variables (discharge, tidal amplitude), on a given sampling date, sites within hydrodynamic zones therefore had identical values. For tidally-averaged discharge, hourly data were reduced to monthly means. In MARSS models, covariates cannot contain missing values, so we used linear interpolation to fill gaps in all covariate time series except for discharge and tidal amplitude (19 of 88 monthly values). Finally, all response variables (log-transformed phytoplankton or zooplankton biomass) and covariate time series were standardized by mean and variance (z-scored) prior to modeling to facilitate model comparison and interpretation across sites and taxa.

MARSS models are state-space extensions of multivariate autoregressive (MAR) models (Ives et al., 2003), allowing for estimation of both process and observational error, and they are robust to missing observations in response variables (Holmes et al., 2012). MAR models simultaneously quantify interaction strengths among taxa as well as the sensitivity of each taxon to environmental covariates (drivers; Ives et al., 2003). We used MARSS models to quantify relationships between environmental drivers and phytoplankton or zooplankton biomass and to determine how these relationships varied among hydrodynamic zones within the DWSC (Questions 1–2). We also quantified the relative importance of environmental drivers and trophic interactions on phytoplankton and zooplankton biomass (Question 3). MARSS models are described by two parts. The first, a process model, describes changes in the true, but unobserved, states of nature over time:

$$\mathbf{x}_t = \mathbf{B}\mathbf{x}_{t-1} + \mathbf{C}\mathbf{c}_{t-h} + \mathbf{w}_t, \quad (2)$$

$\mathbf{x}_t$  is a  $j \times 1$  vector of phytoplankton biovolume or zooplankton biomass at time  $t$  for each of the stations;  $j = 20$ –50 time series depending on the number of taxa

in the model (e.g., phytoplankton, zooplankton, or both). The diagonal elements of the  $j \times j$  matrix **B** determine the degree of mean-reversion of each state process (i.e., density dependence). We allowed each phytoplankton and zooplankton taxon to have a unique estimate of mean reversion. The off-diagonal elements of **B** contain estimates for species interactions (ex., effect of species A on species B's per-capita growth rate). The  $j \times k$  matrix **C** contains the effects of environmental drivers (covariates) measured at time  $t - h$  ( $h = 0$  for this analysis), which are contained in the  $k \times 1$  vector  $\mathbf{c}_{t-h}$ , where  $k$  is the number of covariate time series. The  $j \times 1$  vector  $\mathbf{w}_t$  contains process errors, which are distributed as a multivariate normal with mean vector  $\mathbf{0}$  and covariance matrix **Q**. Following preliminary modeling, we structured **Q** to allow taxon-specific variance and covariance.

The second part of a state-space model is the observation equation, which relates the observed data to the unobserved state processes:

$$\mathbf{y}_t = \mathbf{Z}\mathbf{x}_t + \mathbf{v}_t. \tag{3}$$

The  $i \times 1$  vector  $\mathbf{y}_t$  contains the observed phytoplankton biovolume or zooplankton biomass (logged, z-scored) at time  $t$ ;  $i = 20-50$ . The matrix **Z** maps each of the observed time series onto each of the hidden states in  $\mathbf{x}_t$ —in this analysis we assume plankton dynamics at each station behave as independent processes; thus, **Z** is an identity matrix, and  $\mathbf{y}_t$  and  $\mathbf{x}_t$  have the same dimensions. The  $i \times 1$  vector  $\mathbf{v}_t$  contains the observation errors, which are distributed as a multivariate normal with mean vector  $\mathbf{0}$  and covariance matrix **R**. We assumed

observation error differed between phytoplankton and zooplankton, but that within each group, observation error was equal across all sites because sampling was done consistently.

We tested three sets of MARSS models: the first set investigates environmental drivers of monthly phytoplankton biovolume (Model 1), the second set investigates environmental drivers of monthly zooplankton biomass (Model 2), and the third set investigates phytoplankton–zooplankton trophic interactions (Model 3). For Model 1, we tested for effects of the following environmental drivers on phytoplankton: turbidity (Nephelometric Turbidity Units [NTU]), water temperature ( $^{\circ}\text{C}$ ), normalized tidal amplitude, tidally averaged discharge (cfs), nitrate ( $\text{mg N L}^{-1}$ ), and phosphate ( $\text{mg P L}^{-1}$ ). For Model 2, we tested for effects of turbidity, water temperature, normalized tidal amplitude, tidally averaged discharge, total phytoplankton biovolume ( $\mu\text{m}^3 \text{L}^{-1}$ ), and chlorophyll *a* ( $\mu\text{g L}^{-1}$ ). For Model 3, we only included environmental drivers that significantly improved model fit to the plankton data in Models 1 and 2. Due to the large number of estimated model parameters, we did not test for interactive effects of environmental drivers. For each set of models, we explicitly tested whether effects of environmental drivers or species interactions differed among taxa and spatially among the three hydrodynamic zones, by modifying elements within the **B** and **C** matrices in Equation 2. We include more detail for each set of models below.

Models 1 and 2: We first fitted single-covariate models and compared them with a no-covariate null model. We compared three different structures of **C** in Equation 2 (see Table 1), corresponding to the following hypotheses: (1) all phytoplankton (or zooplankton) taxa across all

**TABLE 1** Details of multivariate autoregressive state space (MARSS) model structure for Model 1 (drivers of phytoplankton), Model 2 (drivers of zooplankton), and Model 3 (phytoplankton–zooplankton interactions).

Model name	Model version	Taxa	Time series	B: Diagonal terms	B: Off-diagonal terms	C: Estimates per covariate
Model 1 (Phytoplankton drivers)	Shared	3	30	3	0	1
	Taxon specific	3	30	3	0	3
	Taxon + zone specific	3	30	3	0	9
Model 2 (Zooplankton drivers)	Shared	2	20	2	0	1
	Taxon specific	2	20	2	0	2
	Taxon + zone specific	2	20	2	0	6
Model 3 (Phytoplankton–zooplankton interactions)	No interaction	5	50	5	0	9; 15
	Taxon specific	5	50	5	12	9; 15
	Taxon + zone specific	5	50	5	36	9; 15

*Note:* For each model version we report the no. taxa included in the model, the total no. observed time series (no. sites  $\times$  no. taxa), and the structure of the **B** and **C** matrices (see Equation 2). For **B**, we report the no. unique diagonal (i.e., mean reversion) and off-diagonal (i.e., species interactions) terms that were estimated. For **C**, we report the no. unique parameter estimates per covariate. Notes: **Q**, **R**, and **Z** structures did not differ among model versions. The dimensions of **B** and **C** did not vary among model versions, only the no. unique matrix elements differed. For Model 3, the no. of unique parameter estimates per covariate differed between covariates (9 vs. 15) because we assumed that phosphate and nitrate affected only phytoplankton taxa; thus, we did not estimate effects of these covariates for zooplankton.



sites share a common relationship with the environmental drivers (“shared”), (2) each taxon has a unique relationship with environmental drivers (“taxon-specific”), and (3) each taxon within each hydrodynamic zone has a unique relationship with the environmental drivers (“taxon + zone specific”). In the “shared” version of each model, a single covariate effect is estimated for all the observed time series. In the “taxon-specific” model version, all the observed time series for a given taxon (across all 10 sites) share the same covariate effect estimate. In the “taxon + zone specific” model version, for each taxon, all the sites within each hydrodynamic zone share the same covariate effect estimate (Table 1). Following the single-covariate modeling, we fitted models with multiple environmental covariates as follows: only covariates that significantly improved model fit relative to the no-covariate null model were included in multiple-covariate models. We started with the covariate that most improved model fit and successively included additional covariates if doing so significantly improved model fits compared to the simpler model. For all versions of Models 1 and 2, we estimated the degree of mean reversion (diagonal elements of **B**, see Table 1) for each taxon, but we did not include interactions between taxa (off-diagonal elements of **B**).

Model 3: For the zooplankton-phytoplankton species interaction models, we first fitted no-covariate models with three different structures of **B** in Equation 2 (see Table 1), corresponding to the following hypotheses: no interactions between zooplankton and phytoplankton (“no interactions,” e.g., off-diagonal elements of **B** are zero), unique interactions between each zooplankton and phytoplankton taxon (“taxon-specific”), and unique interactions between each zooplankton and phytoplankton taxon in each hydrodynamic zone (“taxon + zone specific”). We did not include competitive interactions between different zooplankton or phytoplankton taxa in models. After determining the best structure of **B**, we constructed a final model by including the set of covariates that best explained phytoplankton and zooplankton dynamics in Models 1 and 2.

Models were fit to the data using maximum likelihood via an expectation-maximization algorithm run for 5000 iterations, using the “MARSS” package

(Holmes et al., 2018) for the R software (R Core Team, 2020). We compared model fits using Akaike’s information criterion adjusted for small sample size ( $AIC_c$ ; Burnham & Anderson, 2002). A difference in  $AIC_c$  ( $\Delta AIC_c$ ) > 5 between models suggests moderate support for the model with the lower  $AIC_c$ ;  $\Delta AIC_c$  > 10 shows strong support. For the best-fitting model in each set, we calculated “one-step-ahead” conditional  $R^2$  for each phytoplankton and zooplankton time series, defined as the proportion of variation from time  $t - 1$  to  $t$  that can be explained by the model (as in Walsh et al., 2018).

## RESULTS

### Spatial and seasonal patterns in chemistry and plankton biomass

Spatial patterns in water isotopes, water temperature, specific conductance, turbidity, nutrient concentrations, and phytoplankton and zooplankton biomass reflected changes in hydrodynamic exchange and water residence time along the DWSC (Figure 1; Table 2). Both  $\delta^{18}\text{O-H}_2\text{O}$  and  $\delta^2\text{H-H}_2\text{O}$  were more enriched in the landward reaches (Table 2; Appendix S1: Figure S3), consistent with longer residence time and greater evaporation (Downing et al., 2016). Surface water temperatures were slightly but significantly warmer in the NE zone relative to seaward reaches ( $+2^\circ\text{C}$ ,  $F_{2,717} = 12.37$ ,  $p < 0.001$ , Table 2). Specific conductance increased significantly from seaward to landward stations ( $F_{2,717} = 112.1$ ,  $p < 0.001$ ; HE:  $356 \pm 742 \mu\text{S cm}^{-1}$ , LE:  $555 \pm 150$ , NE:  $952 \pm 145$ ), reflecting greater water residence time and evaporation (Lenoch et al., 2021; Stumpner, Burau, & Forrest, 2020). Turbidity was significantly higher in the LE zone than the HE or NE zones ( $F_{2,717} = 38.5$ ,  $p < 0.001$ ), but was frequently high in adjacent stations (CM 56, 70; Figure 1).

Nitrate concentrations were significantly lower in the NE zone than in the HE or LE zones ( $F_{2,717} = 165.2$ ,  $p < 0.001$ ). Ammonium concentrations were significantly lower in the LE and NE zones than in the HE zone ( $F_{2,717} = 481.6$ ,  $p < 0.001$ ). Phosphate concentrations

**TABLE 2** Environmental conditions, water chemistry, and plankton biovolume or biomass in each hydrodynamic exchange zone during the study period (2012–2019, 74 sampling dates).

Zone	$\delta^2\text{H-H}_2\text{O}$ (‰)	$\delta^{18}\text{O-H}_2\text{O}$ (‰)	Temp (°C)	Turb (NTU)	$\text{NO}_3$ (mg N L <sup>-1</sup> )	$\text{NH}_4$ (mg N L <sup>-1</sup> )	$\text{PO}_4$ (mg P L <sup>-1</sup> )	$\text{SiO}_2$ (mg Si L <sup>-1</sup> )	Cond ( $\mu\text{S cm}^{-1}$ )	Chl <i>a</i> ( $\mu\text{g L}^{-1}$ )	Phyto ( $10^9 \mu\text{m}^3 \text{L}^{-1}$ )	Zoop ( $\mu\text{g dw L}^{-1}$ )
HE	-73.4 (2.8)	-10.1 (0.5)	17.3 (4.6)	21.9 (29.8)	0.32 (0.17)	0.14 (0.08)	0.06 (0.02)	7.45 (1.09)	356.2 (742.8)	2.4 (3.3)	1.91 (4.45)	12.63 (14.08)
LE	-60.5 (3.9)	-7.8 (0.8)	18.1 (4.8)	33.1 (17.4)	0.30 (0.18)	0.02 (0.01)	0.10 (0.02)	7.46 (0.83)	555.5 (150.8)	3.5 (2.1)	1.19 (1.94)	26.29 (25.06)
NE	-50.8 (3.5)	-6.0 (0.8)	19.3 (5.4)	14.0 (10.3)	0.11 (0.12)	0.02 (0.01)	0.10 (0.02)	7.48 (0.59)	953.0 (145.2)	4.9 (3.9)	1.07 (2.03)	63.69 (67.03)

Note: Means (and standard deviations) are reported for each hydrodynamic zone (HE, high exchange; LE, low exchange; NE, no exchange).

Abbreviations: Chl *a*, chlorophyll *a*; Cond, specific conductance; Phyto, phytoplankton; Temp, temperature; Turb, turbidity; Zoop, zooplankton.

were significantly higher in landward reaches compared with the HE zone ( $F_{2,717} = 270.6, p < 0.001$ ). Silica concentrations did not vary spatially ( $F_{2,717} = 0.04, p > 0.5$ ). Chlorophyll *a* concentrations increased significantly from seaward to landward reaches ( $F_{2,717} = 38.89, p < 0.001$ ), whereas total phytoplankton biovolume decreased ( $F_{2,717} = 5.56, p < 0.01$ ). Zooplankton biomass increased from seaward to landward reaches ( $F_{2,717} = 101.6, p < 0.01$ ).

GAMM's fit to month of year showed distinct seasonal patterns in most environmental variables within the DWSC (Figure 2), though seasonal phenology also varied among zones (e.g., discharge, turbidity, ammonium), and some variables lacked distinct seasonality (e.g., phosphate). Tidally averaged discharge in the HE zone was highest in winter, reflecting the seasonal hydrology of the Sacramento River, whereas discharge had no distinct seasonality in the

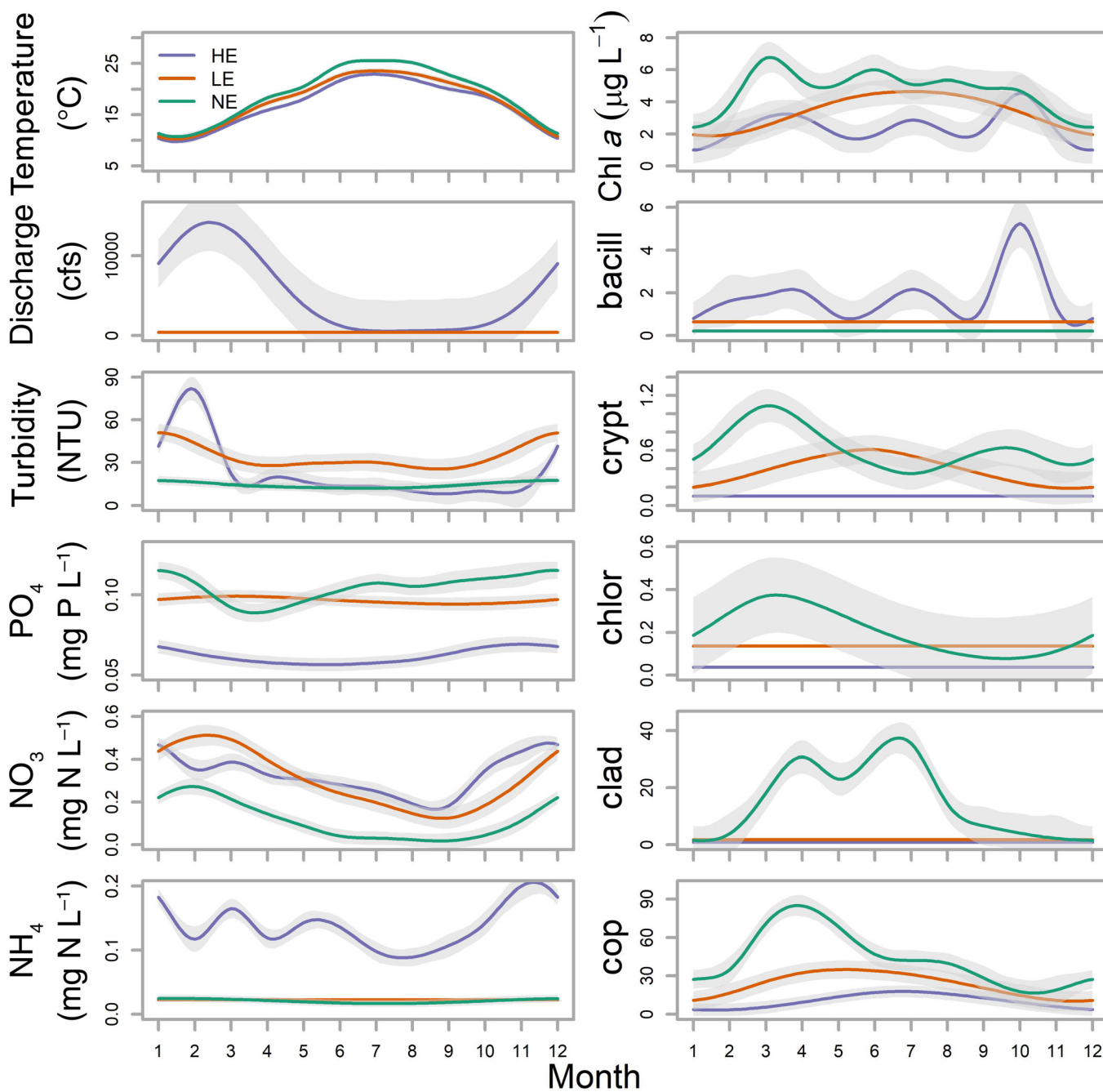


**FIGURE 2** Left column: Generalized additive mixed models (GAMM's) of environmental variables fitted to month in each hydrodynamic zone (solid lines; HE, high exchange; LE, low exchange; NE, no exchange) with 95% confidence intervals (CI) (gray shaded areas). Tidally averaged discharge from CM45 is shown for the HE zone, and CM 54 for the LE zone. Right column: Seasonal GAMM's of chlorophyll *a* concentration ( $\mu\text{g L}^{-1}$ ), phytoplankton biovolume ( $10^9 \mu\text{m}^3 \text{L}^{-1}$ ; bacill, Bacillariophyta; crypt, Cryptophyta; chlor, Chlorophyta) or zooplankton biomass (units  $\mu\text{g dw L}^{-1}$ ; clad, Cladocera; cop, Copepoda) for each hydrodynamic zone. y-axis scales differ between panels.

landward reaches. Similarly, turbidity in the HE and LE zones was high in winter and low in summer but lacked seasonality in the NE zone. Water temperatures were highest in the summer (June–August), following annual patterns in solar radiation and air temperature. Nitrate concentrations were lower in summer than in other seasons. Chlorophyll *a* concentrations were generally lowest in winter (December–February), but seasonal patterns differed among zones at other times of year.

## Phytoplankton community composition

Phytoplankton community composition varied spatially, shifting from predominantly bacillariophytes (diatoms) in the HE and LE zones to predominantly cryptophytes in the landward NE zone (Figure 3A; Appendix S1: Figure S4). Chlorophytes contributed a minor proportion of total biovolume except in the NE zone. On average, cyanophytes, pyrrophytes, euglenophytes, and chrysophytes were minor components of community composition in all zones (combined <10% of total biovolume). GAMM's fit to month

of year showed differences in seasonality among phytoplankton taxa and between hydrodynamic zones (Figure 2). Bacillariophyte biovolume in the HE zone had distinct peaks in spring, summer, and autumn but lacked seasonality in the other two zones. Seasonal patterns in cryptophyte or chlorophyte biovolume were also spatially variable; neither had significant seasonal trends in the HE zone, but seasonal trends differed between the LE and NE zones (Figure 2).

In HE zone, bacillariophytes were the dominant phytoplankton taxon (mean 83% of total biovolume across all samples,  $n = 74$  sampling dates), with cryptophytes making up 11%, chlorophytes 2%, cyanophytes 2%, and less than 1% each for pyrrophytes, euglenophytes, and chrysophytes. The most frequently detected bacillariophyte species in the HE zone were *Cocconeis placentula* and *Synedra ulna* (detection frequency 98%, 99%), but *Entomoneis* sp., *Melosira varians*, and *Aulacoseira granulata* had the highest median biovolumes when present (only species detected on >25 dates are reported; Appendix S1: Table S1). The most commonly detected cryptophytes in the HE were *Rhodomonas* sp. (59% detection frequency) and *Cryptomonas* sp. (53%),

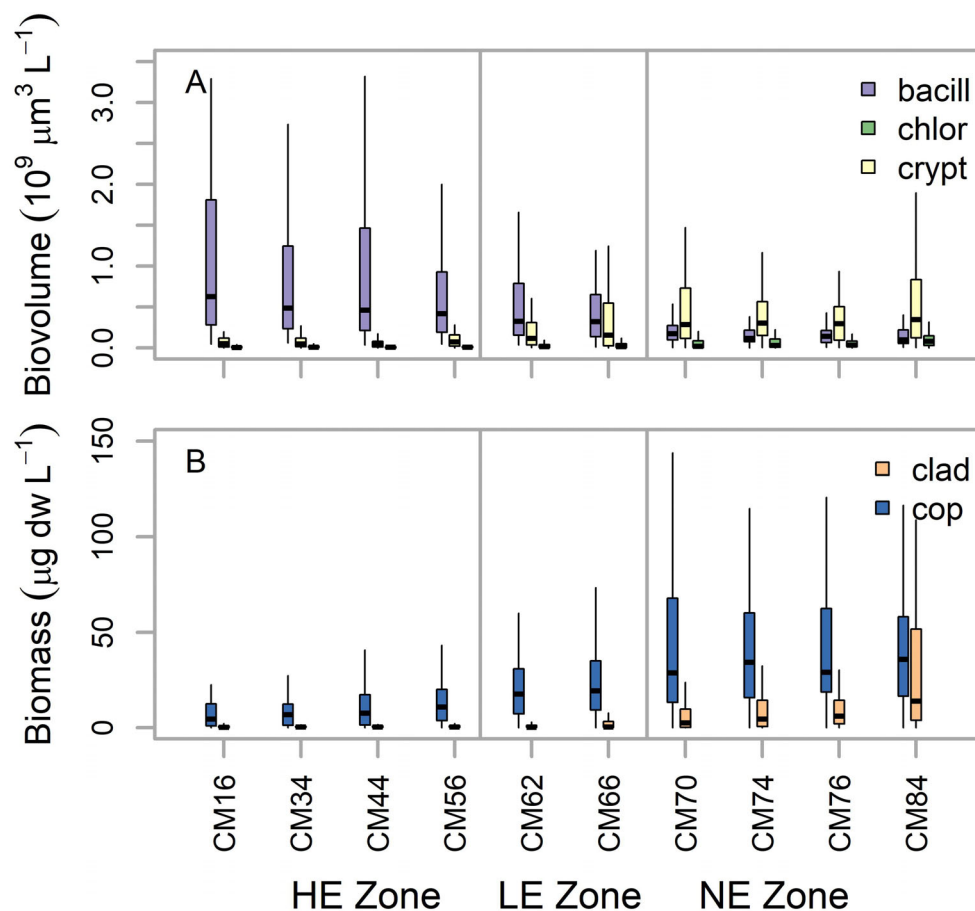


**FIGURE 3** Biovolume or biomass of dominant phytoplankton (A) and zooplankton (B) taxa at each sampling station. Stations are ordered from seaward to landward, as in Figure 1. bacill, Bacillariophyta; chlor, Chlorophyta; clad, Cladocera; cop, Copepoda; crypt, Cryptophyta.

which also had the highest median biovolumes, and *Chlorella* sp. was the only chlorophyte detected consistently (33% detection frequency).

In the LE zone, bacillariophytes were dominant (59% of total biovolume), but cryptophyte and chlorophyte biovolumes were relatively higher (33%, 5%) than in the HE zone. The most frequently detected bacillariophyte species were *Cocconeis placentula* (95% detection frequency), *Thalassiosira* sp. (68%), and *Synedra ulna* (59%), whereas the species with the highest median biovolumes when present were *Thalassiosira* sp. and *Aulacoseira granulata*. The most commonly detected cryptophytes in the LE zone were *Rhodomonas* sp. (detection frequency 57%), and *Cryptomonas erosa* (39%)—in addition to these species, *Plagioselmis nannoplanctica* had the highest median biovolume when present. The most frequently detected chlorophytes were *Chlamydomonas* sp. (34%) and *Chlorella* sp. (20%), and these species also had the highest median biovolumes when present.

In the NE zone, cryptophytes were the dominant taxa (53% of total biovolume), followed by bacillariophytes (27%), and chlorophytes (12%). The most frequently detected cryptophytes were *Cryptomonas* sp. (67% detection frequency), *Cryptomonas erosa* (60%), and *Rhodomonas* sp. (64%), while the species with highest median biovolumes when detected were *Rhodomonas* sp., *Rhodomonas lacustris*, and *Plagioselmis nannoplanctica*. Similar to the LE zone, the most frequently detected bacillariophytes in the NE zone were *Cocconeis placentula* (89% detection frequency), *Thalassiosira* sp. (68%), and *Synedra ulna* (39%), whereas the species with highest median biovolumes when present were *Thalassiosira* sp., *Cyclotella meneghiniana*, and *Aulacoseira* sp. The most frequently detected and highest biovolume chlorophytes were *Chlamydomonas* sp. (77% detection frequency), *Chlorella* sp. (32%), and *Chlamydomonas globosa* (31%).

The proportion of total phytoplankton biovolume made up by species classified as “low quality” was higher in the HE zone than in the landward zones (Appendix S1: Figure S5). Low quality species made up 22% of total phytoplankton biovolume, on average, in the HE zone, 7% in the LE zone, and 1% in the NE zone. Low quality phytoplankton were primarily bacillariophytes (*Aulacoseira* sp., *Melosira varians*), though occasionally cyanobacteria (*Anabaena* sp., *Aphanizomenon* sp., *Microcystis* sp.) or pyrophytes (*Peridinium* sp.) contributed a large proportion of total phytoplankton biovolume (Appendix S1: Figure S5).

## Zooplankton community composition

Copepods dominated zooplankton biomass throughout the DWSC (>75% of total biomass across all sampling dates),

but cladocerans were a relatively greater proportion of the total biomass in the landward NE zone (mean 23%) than in the HE and LE zones (13% and 5% respectively; Figure 3B; Appendix S1: Figure S4). All other taxa made up less than 5% of total biomass in all three zones (Rotifera, Ostracoda, Gastropoda, Bivalvia, Cnidaria). The seasonal phenology of zooplankton biomass differed between copepods and cladocerans, with copepods tending to attain high biomass earlier in spring than cladocerans (April–May; Figure 2). Within taxa, phenology also differed between zones (Figure 2). Copepods in the HE zone peaked in early summer (June, July), whereas copepod biomass increased earlier, in spring in the LE and NE zones (March–April), and remained elevated throughout summer. Cladoceran biomass in the HE and LE zones had no distinct seasonal pattern, whereas cladocerans in the NE zone increased in spring and remained high throughout summer (April–August).

In the HE zone, the most frequently detected and highest biomass copepod species were the calanoid copepods *Pseudodiaptomus forbesii* and *Sinocalanus doerri* (89% detection frequency for both species; Appendix S1: Table S2). The most common cladoceran species were *Bosmina longirostris* (97% detection frequency) and *Chydorus sphaericus* (61%), though when present, *Daphnia* sp. had the highest median biomass. The only commonly detected rotifer was *Asplanchna* sp. (>25 sampling dates, 38% detection frequency).

In the LE zone, the calanoid copepod species *Sinocalanus doerri* (100%) and *Pseudodiaptomus forbesii* (93%), were most frequently detected and had the highest median biomass. The most commonly detected cladoceran species was *Diaphanosoma brachyurum* (46% detection frequency).

In the NE zone, as in the HE and LE zones, calanoid copepods *Sinocalanus doerri* and *Pseudodiaptomus forbesii* remained the most commonly detected copepod species (72%, 64%). *Bosmina longirostris* (95%) and *Diaphanosoma brachyurum* (75%) were the most frequently detected cladoceran species, but *Diaphanosoma brachyurum*, *Daphnia* sp., and *Daphnia parvula* had the highest median biomass when present.

## Environmental drivers of phytoplankton (Model 1)

Turbidity, phosphate, and water temperature were the three abiotic drivers that most improved model fits to the log-phytoplankton data ( $\Delta AIC_c > 20$  relative to no-covariate model), followed by discharge, nitrate, and tidal amplitude ( $\Delta AIC_c > 5$ ). Including nitrate or tidal amplitude as covariates only slightly improved model fit

relative to the no-covariate model ( $\Delta AIC_c > 2$ ). For all single-covariate models, “taxon + zone specific” effects of environmental drivers were the best **C** structure, compared with “taxon-specific” or “shared,” though for nitrate and tidal amplitude, support for zone-specific effects was weak ( $\Delta AIC_c > 2$ ). The best-fitting multiple-covariate model included all covariates ( $AIC_c = 5089$ ;  $\Delta AIC_c > 70$  compared to no-covariate model; see Appendix S1: Table S3 for parameter estimates and standard errors), though this model was not significantly better than a model lacking nitrate and tidal amplitude ( $\Delta AIC_c < 4$  between models).

The effects of environmental drivers differed both among taxa and among the hydrodynamic zones (Figure 4, estimates are from best-fitting multiple-covariate model). Bacillariophyte biovolume was positively associated with turbidity and discharge in all zones and negatively associated with phosphate concentration in the HE and LE zones. In the NE zone, bacillariophyte biovolume was negatively associated with nitrate concentration. Water temperature and tidal amplitude did not have significant effects on bacillariophytes in any zone.

Cryptophytes, like bacillariophytes, were positively associated with discharge and negatively associated with phosphate, though effects were only significant in the NE zone (Figure 4 row 2). Unlike bacillariophytes, cryptophytes were negatively associated with turbidity (HE zone only) and positively associated with water temperature (LE zone). Cryptophytes were the only taxa that showed a significant (negative) relationship with tidal amplitude, but only within the NE zone.

Chlorophytes had positive associations with water temperature (all zones) and nitrate concentrations (HE, NE) and negative associations with phosphate (HE, NE; Figure 4 row 3). Chlorophyte biovolume was not significantly related to turbidity or discharge. Similar to bacillariophytes, tidal amplitude had a positive effect on chlorophytes, but only in the HE zone.

Even for the best fitting model, conditional  $R^2$  (one step ahead) was low for all three phytoplankton taxa: environmental covariates best explained temporal dynamics of chlorophytes (among-site mean 37%; among-site range 23%–47%), followed by cryptophytes (21%; 15%–28%) and bacillariophytes (15%; 7%–24%).

## Environmental drivers of zooplankton (Model 2)

When included as single covariates, water temperature, turbidity, and discharge were the drivers that most improved model fit to the zooplankton data ( $\Delta AIC_c > 40$ ), followed by tidal amplitude and chlorophyll *a* ( $\Delta AIC_c > 5$ ). Including total phytoplankton biovolume (logged) did not

significantly improve model fit relative to the no-covariate model ( $\Delta AIC_c < 2$ ). For all covariate models, “taxon + zone specific” effects of environmental drivers were the best **C** structure. The best-fitting multiple covariate model included all covariates except for total phytoplankton biovolume and tidal amplitude ( $AIC_c = 3143$ ;  $\Delta AIC_c > 300$  relative to no-covariate model).

Warm water temperatures were associated with greater zooplankton biomass, though the strength of the effect differed among zones for each taxon (Figure 4; Appendix S1: Table S4). Higher turbidity was associated with lower copepod biomass (Figure 4 row 5), whereas cladoceran biomass was not related to turbidity. Discharge had a generally negative effect on zooplankton across zones, though the effect was stronger for cladocerans than copepods. Chlorophyll was negatively associated with cladoceran biomass in the HE and LE zones, but weakly positively associated with both cladoceran and copepod biomass in the NE zone. Tidal amplitude had a positive effect on cladocerans in the LE and NE zones, but no effect in the HE zone, whereas copepods showed the opposite—greater tidal amplitude was negatively associated with copepod biomass in the LE and NE zones. Conditional  $R^2$  (one step ahead) for the best multiple-covariate model was similar for copepods (among-site mean 39%; among-site range 15%–67%) and cladocerans (32%; 9%–46%).

## Phytoplankton–zooplankton interactions (Model 3)

There was strong support in the data for trophic interactions between zooplankton and phytoplankton ( $\Delta AIC_c > 40$  compared to the “no interactions” null model, Table 3), and interaction strengths between pairs of taxa varied significantly among the three hydrodynamic zones (Figure 5; Table 3;  $\Delta AIC_c > 150$  compared to species interaction model lacking spatial variation). Cryptophytes had strong positive associations with both cladocerans and copepods, whereas bacillariophytes and chlorophytes had weak or no bottom-up effects on either zooplankton taxa, and occasionally had negative effects (Appendix S1: Table S5). In general, cladocerans had stronger negative associations with phytoplankton than did copepods. The strength of top-down interactions between cladocerans and phytoplankton increased in the landward direction, concurrently with increases in water residence time and cladoceran biomass (Figure 3B): cladocerans had strong negative effects on all three phytoplankton taxa in the NE zone, a negative effect on cryptophytes in the LE zone, but no effect on phytoplankton in the HE zone. Copepods had a negative but non-significant effect on bacillariophytes in

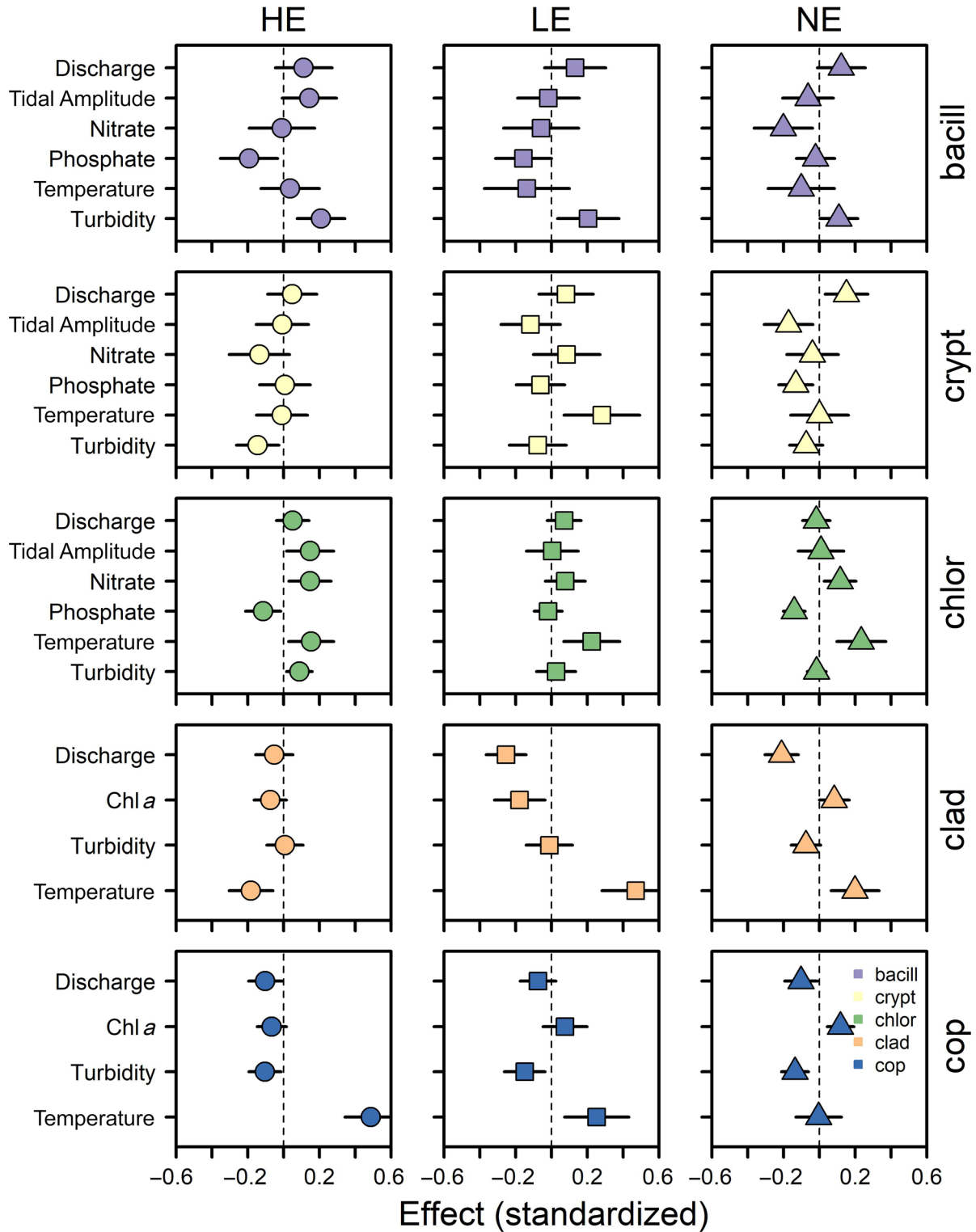


**FIGURE 4** Standardized effects (with 95% CI; x-axes) of environmental covariates (y-axes) on the dominant phytoplankton and zooplankton taxa (rows; bacill, Bacillariophyta; crypt, Cryptophyta; chlor, Chlorophyta; clad, Cladocera; cop, Copepoda) in each hydrodynamic zone (columns; HE, high exchange; LE, low exchange; NE, no exchange). CI that span zero imply a non-significant effect. Only covariates that significantly improved model fits relative to a no-covariate null model are shown. Effects are the maximum likelihood estimates from the best-fitting multiple-covariate phytoplankton or zooplankton model (Models 1 and 2). Point colors correspond to taxa and point symbols correspond to hydrodynamic zones.

**TABLE 3** The six considered species-interaction model versions (Model 3;  $n = 3450$ ), the number of estimated model parameters ( $k$ ), Akaike information criterion for small sample sizes ( $AIC_c$ ), and the difference in  $AIC_c$  compared with the best-fitting model ( $\Delta AIC_c$ ).

Model version	$k$	$AIC_c$	$\Delta AIC_c$
Taxon + zone-specific interactions + covariates	116	8145	0
Taxon-specific interactions + covariates	92	8208	63
No interactions + covariates	80	8250	105
Taxon + zone-specific interactions	53	8388	243
Taxon-specific interactions	29	8572	427
No interactions	17	8614	469

the HE zone, and a weak negative effect on chlorophytes in the LE zone, but had positive effects on phytoplankton biovolume in the NE zone.

Conditional  $R^2$  (one step ahead) for the best species-interaction model was greatest for copepods (among-site mean 45%; among-site range 22%–73%; Appendix S1: Table S6; Appendix S1: Figure S6), cladocerans (31%; 6%–52%), and chlorophytes (34%; 21%–47%), and least for cryptophytes (20%; 8%–35%) and bacillariophytes (18%; 8%–32%). Including species interactions in models with covariates increased one-step-ahead  $R^2$  more for zooplankton time series than for phytoplankton (+10% vs. +2% average increase in  $R^2$ ). Within each taxonomic group, including species interactions improved  $R^2$  more in sites within the NE zone than in the LE or HE zones. Within each taxonomic group, conditional  $R^2$  varied among sites across the DWSC (Appendix S1: Figure S6). Conditional  $R^2$  for copepod time series was highest in the HE zone and declined in the landward direction, whereas for cladocerans,  $R^2$  was lowest near the transition from the HE zone to the LE zone (CM 44, 56, 62).  $R^2$  for cryptophyte and chlorophyte time series showed slight spatial variation along the DWSC, but  $R^2$  was uniformly low for bacillariophytes regardless of location.

## DISCUSSION

### Overview

Few estuarine studies explicitly consider how spatial variation in residence time mediates effects of both biotic and abiotic drivers of phytoplankton and zooplankton biomass. We showed that controls on zooplankton and phytoplankton biomass in a tidal freshwater portion of the SFE varied significantly among habitats structured by hydrodynamics and differed between taxonomic groups

(Figures 4 and 5). Spatial variation in water exchange and water residence time, turbidity, nutrient concentrations, and plankton community composition resulted in different temporal drivers of zooplankton and phytoplankton biomass among habitats. A model with only abiotic drivers explained more variation in phytoplankton and zooplankton dynamics than a model including only trophic interactions (Table 3); however, individual phytoplankton–zooplankton interactions were generally larger than effects of most abiotic drivers when all were included in the same model. Interactions between zooplankton and phytoplankton were strongest in landward reaches with the longest residence times (weeks to months; Stumpner, Burau, & Forrest, 2020) and the highest zooplankton biomass (Figure 1, Table 2), but were also taxon-specific.

Differences in pelagic communities and food web structure among estuaries are often driven by regional variation in climate and watershed processes, as well as the degree of anthropogenic influence (Donázar-Aramendía et al., 2019; McClelland & Valiela, 1998; Park & Marshall, 2000), whereas variation within estuaries is often attributed to longitudinal salinity gradients (Vinagre & Costa, 2014). Though numerous studies have characterized variability in physical and chemical drivers of community structure, our results demonstrate that trophic interactions and their relative strengths vary with water residence time, contributing to food web heterogeneity within estuaries at spatial scales smaller than the freshwater to marine transition. Consequently, food web studies may benefit from accounting for smaller-scale hydrodynamic variation within pelagic habitats of estuaries—the concept of “exchange zones” as we have used here is a useful one for defining pelagic habitats in terminal channels and sloughs (Stumpner, Burau, & Forrest, 2020). Characterizing trophic interactions in the context of hydrodynamic variability will facilitate comparisons across estuaries, because among-estuary patterns in food web structure may be obscured by high within-estuary variation (França et al., 2011; Ghosh & Bhadury, 2019; Pihl et al., 2002).

### Biomass, community composition, and trophic interactions linked to hydrodynamics

The residence time of aquatic ecosystems, which is related to water exchange rate, controls both bottom up and top down food-web processes, leading to complex relationships with plankton biomass (Lucas & Thompson, 2012). Long residence times in aquatic habitats can either promote phytoplankton biomass by increasing production and retention (Glibert, Dugdale, et al., 2014; Howarth et al., 2000; Stumpner, Bergamaschi, et al., 2020), or decrease

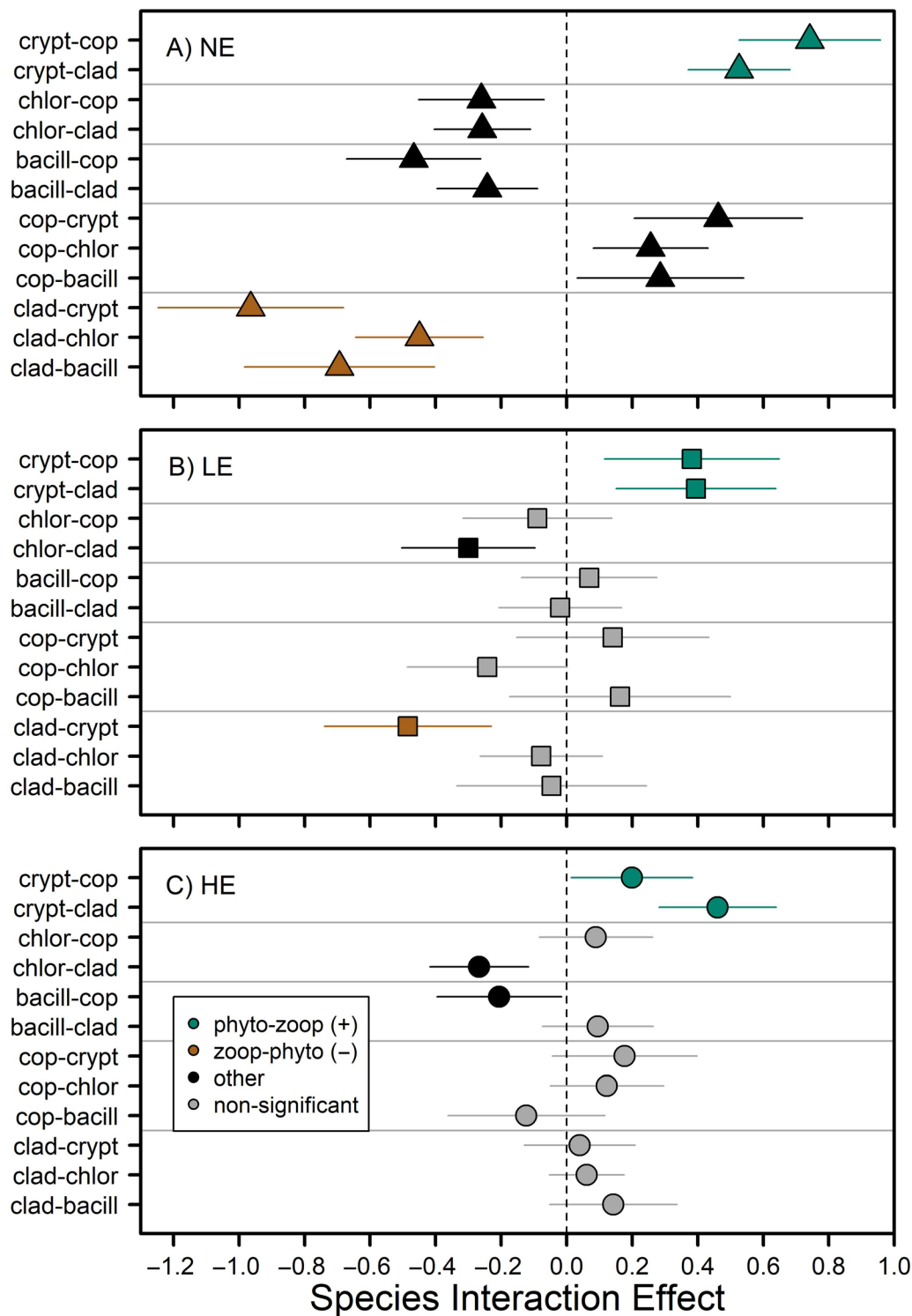


**FIGURE 5** Standardized effects (with 95% CI; x-axes) of phytoplankton on zooplankton (“bottom-up effects”; green) and zooplankton on phytoplankton (“top-down”; brown) in each hydrodynamic zone (A–C). Black shapes show negative effects of phytoplankton on zooplankton or positive effects of zooplankton on phytoplankton (“other”). Point shapes correspond to hydrodynamic zones as in previous figures. 95% CI spanning zero suggest that estimates of species interactions are non-significant—non-significant effects are shown in gray. Y-axis labels show all estimated interactions (“taxa1-taxa2” refers to the effect of taxa 1 on taxa 2; bacill, Bacillariophyta; crypt, Cryptophyta; chlor, Chlorophyta; clad, Cladocera; cop, Copepoda). Effects are maximum likelihood estimates from the best-fitting species-interaction model with covariates (Model 3). HE, high exchange; LE, low exchange; NE, no exchange.



phytoplankton biomass by enhancing zooplankton or benthic grazing (and biomass; Kimmerer & Thompson, 2014; Pace et al., 1992) or particle settling (Lucas et al., 2009). Positive associations between residence time and phytoplankton biomass have been observed in the SFE and other estuaries (Gameiro et al., 2004; Schuchardt & Schirmer, 1991; Stumpner, Burau, & Forrest, 2020). However, we measured lower phytoplankton biovolume in the landward habitats (Table 2), and our models showed increasingly strong top-down control by zooplankton in landward areas with longer residence times (Figure 5). The decrease in phytoplankton biovolume we observed from seaward to landward reaches, concurrent with increased light availability (lower turbidity), decreased dissolved inorganic N, and increased zooplankton biomass (Figure 1C,D,G), suggest both high phytoplankton productivity (Loken et al., 2022) and strong top-down control by zooplankton in landward reaches. While in many estuarine habitats mesozooplankton biomass or grazing rates are likely too low for top-down control of phytoplankton (Lionard et al., 2005; Lopez et al., 2006), terminal channels with long residence times and high zooplankton densities may prove an exception (Montgomery et al., 2017; Young, Feyrer, et al., 2021; Young, Howe, et al., 2021).

In addition to controlling biomass, residence time influences phytoplankton and zooplankton community composition in estuaries and rivers, with important implications for pelagic food webs. Long residence times favor motile phytoplankton taxa (ex., cryptophytes) that can maintain their position within the euphotic zone, over larger cells prone to settling (ex., centric diatoms), which thrive in turbid, turbulent systems due to rapid growth rates and tolerance for low light (Reynolds & Descy, 1996). We observed a seaward to landward shift from diatoms to flagellated cryptophytes concomitant with increasing residence time (Figure 3A), matching previous findings within the SFE (Stumpner, Bergamaschi, et al., 2020). Similar shifts in phytoplankton communities associated with residence time occur in large rivers, for example between main channels and backwaters (Manier et al., 2021). Several estuarine studies, including ours, have shown increases in cladoceran biomass corresponding to longer mean residence time (Montgomery et al., 2017; Young, Feyrer, et al., 2021). These spatial differences in both producer and grazer communities could generate spatial differences in food web structure and trophic efficiency across habitats.

### Importance of specific trophic interactions

The importance of specific zooplankton–phytoplankton interactions in our models, coupled with weak associations between zooplankton and chlorophyll *a* or total

phytoplankton biovolume, suggest that quantifying resource availability within pelagic food webs in estuaries may require sample collection or sensor measurements that distinguish among algal taxa. Cryptophytes had positive effects on both cladocerans and copepods in all zones (Figure 5), despite making up a smaller proportion of total biovolume than bacillariophytes in all but the NE zone. In contrast, bacillariophytes had only weak positive, or even negative, effects on zooplankton, despite a general focus on diatoms as preferred food resources for selective zooplankton grazers such as copepods (Irigoien et al., 2002). A positive effect of cryptophytes on zooplankton has been observed in freshwater environments (ex., Lake Washington, Hampton et al., 2006), and has been ascribed to their high nutritional value and fatty acid content (Brett & Müller-Navarra, 1997; Galloway & Winder, 2015). The lack of significant positive effects of bacillariophytes on zooplankton in our study may in part reflect the coarse taxonomic grouping in our models. Low-quality bacillariophytes such as the chain-forming *Aulacoseira granulata* were occasionally dominant within the HE zone (Appendix S1: Figure S5); thus, grouping these with higher quality species may have obscured trophic relationships with zooplankton. Blooms of *A. granulata* were observed throughout the Delta during summer of 2016, including within our own dataset, yet these blooms were not associated with increases in the dominant calanoid copepod *Pseudodiaptomus forbesi* (Jungbluth et al., 2021). The lack of positive, bottom-up interactions between chlorophytes and zooplankton is more understandable—chlorophytes were always a minor component of total biovolume and exhibited more extreme temporal variation (less mean reversion, diagonal elements of **B** close to 1), suggesting they are an ephemeral resource for grazers. Chlorophytes, which tend to have higher chlorophyll:carbon ratios than bacillariophytes (Deblois et al., 2013), were more dominant in the landward reaches (Figure 3A), which may explain why chlorophyll *a* increased from seaward to landward, whereas both bacillariophyte and total phytoplankton biovolume decreased (Table 2, Figures 1, 3). Chlorophyll *a* concentration was a poor predictor of zooplankton biomass (Figure 4), highlighting its limitations as a proxy of food availability for pelagic grazers (Kimmerer et al., 2018).

Cladocerans appear to be more important grazers than copepods on all three phytoplankton taxa in the landward reaches of the DWSC (Figure 5), potentially reflecting differences in feeding rates or feeding mode (Sommer & Sommer, 2006). In feeding experiments, cladocerans have higher grazing rates on phytoplankton than copepods (Gifford et al., 2007), though rates depend on phytoplankton cell size. Copepods generally select for larger phytoplankton cells than do filter-feeding

cladocerans (Sommer & Sommer, 2006); thus, the lack of top-down effects of copepods on bacillariophytes was somewhat surprising. However, we may have underestimated direct top-down effects of copepods on phytoplankton, because nauplii, early copepodites, and smaller cyclopoid copepods such as *Limnoithona tetraspina* were not effectively sampled by our zooplankton net.

Another plausible explanation for the lack of top-down effects of copepods on phytoplankton is that species such as *P. forbesi*, the dominant copepod in our study system, are omnivorous (York et al., 2014), and may not exert strong top-down control on phytoplankton if they are consuming alternative prey sources such as ciliates (Bowen et al., 2015). In fact, positive associations between copepod and phytoplankton biomass, rather than negative top-down associations, have been shown experimentally and empirically in a wide range of freshwater and marine ecosystems (Hampton et al., 2008; Sommer & Sommer, 2006; Stibor et al., 2004). Because we did not sample microzooplankton, which often exert stronger grazing pressure on phytoplankton than mesozooplankton (Lionard et al., 2005), we cannot directly estimate these food web linkages. However, significant positive associations between copepods and phytoplankton in landward reaches (Figure 5) indicate a well-documented trophic cascade, wherein copepod predation on microzooplankton releases phytoplankton from grazing pressure (Armengol et al., 2017; Sommer & Sommer, 2006).

## Abiotic drivers of phytoplankton and zooplankton

Phytoplankton production in estuaries responds to changes in both light and nutrient availability (Pennock & Sharp, 1986). The SFE receives high nutrient inputs from agricultural and urban sources, with nitrogen and phosphorus generally above limiting concentrations, yet has lower primary productivity than many other estuaries worldwide (Cloern et al., 2014; Jassby et al., 2002). Previous work in the SFE has demonstrated light limitation of phytoplankton productivity due to high turbidity (Alpine & Cloern, 1988; Cloern, 1987), though field studies have shown discrepancies between productivity predicted by light models compared to in situ measurements in certain habitats (Parker et al., 2012; Stumpner, Bergamaschi, et al., 2020). Given this context, we expected to see negative effects of turbidity on phytoplankton, and only weak effects of nitrate in the landward reaches of the DWSC where nitrogen concentrations can become limiting in summer (Loken et al., 2022). However, only cryptophytes showed the expected negative relationship with turbidity (Figure 4), whereas bacillariophyte biomass was positively associated with turbidity in all three zones, and chlorophytes were positively associated in the HE zone. The

positive relationship between turbidity and bacillariophytes may reflect resuspension of particulate matter, including large-bodied phytoplankton cells, during turbid conditions caused by tidal cycles, seasonal hydrology, or ship traffic. Bacillariophytes are larger and prone to settling out of the water column, which may explain why their biovolume increased during periods of higher turbidity. In contrast, cryptophytes are smaller and flagellated, making them less dependent on resuspension to remain in the photic zone, and they had a negative association with turbidity (Figure 4), potentially because the diminished light availability caused by higher turbidity was a more important factor.

Effects of nutrient concentrations on phytoplankton are difficult to interpret at monthly timescale because phytoplankton growth can vary at much shorter intervals (hours–days; Lucas et al., 2006). The direction and magnitude of associations between nitrate and phytoplankton biovolume differed among taxa and varied spatially (Figure 4), whereas phosphate was negatively associated with all taxa. Negative associations between nitrate or phosphate and phytoplankton biovolume likely reflect uptake during growth. Bacillariophytes were negatively associated with nitrate in the NE zone but had no associations in the seaward zones where ammonium concentrations were highest (Figure 1), potentially reflecting suppression of nitrate uptake (Dugdale et al., 2007). Though high ammonium concentrations have been hypothesized as contributing to declines in bacillariophyte biomass in the SFE (Glibert, Wilkerson, et al., 2014), in our study, high ammonium co-occurred with daily tidal exchange and short residence times in the HE zone, complicating our ability to distinguish among potential mechanisms (Ward & Paerl, 2016). Chlorophytes, in contrast with bacillariophytes, were positively associated with nitrate concentration across zones, and nitrate had no significant association with cryptophytes in any zone. Positive associations between nitrate and chlorophytes may reflect the fact that chlorophyte biovolume in the landward reaches is highest in summer, when dissolved inorganic nitrogen concentrations are lower. In situ measurements and incubation experiments suggest nitrogen-limitation in the landward reaches of the DWSC during stratified periods of summer (Loken et al., 2022), but monthly sampling is insufficient to capture rapid phytoplankton blooms in response to nutrient inputs (Dugdale et al., 2007) and short-time scale variation in hydrodynamics (Lenoch et al., 2021). Overall, the associations of nitrate and phosphate with phytoplankton were small and frequently non-significant, suggesting that at seasonal and inter-annual time scales other drivers were more important.

Water temperature was positively associated with phytoplankton biovolume, but the relationship was only significant for chlorophytes and for cryptophytes in the

LE zone. The positive association between temperature and chlorophyte biovolume agrees with prior work demonstrating greater chlorophyte biovolume in the SFE during drought years with higher water temperatures (Lehman, 2000). However, seasonal variation in water temperature was much greater than spatial differences among sites (Figure 2); therefore, we considered water temperature a seasonal proxy in our models (Hampton et al., 2006; Walsh et al., 2018).

While our models supported the hypothesis of both taxon-specific and habitat-specific drivers of phytoplankton, the combined set of abiotic drivers and trophic interactions explained little temporal variation in phytoplankton biovolume (Appendix S1: Table S6, Figure S6), particularly for bacillariophytes. This is likely due to the coarse time-scale of our sampling relative to phytoplankton doubling rates (Loken et al., 2022). While other studies in the SFE did not show substantial variation in primary production rates or community composition at weekly to biweekly time scales (Kimmerer et al., 2012), monthly sampling is insufficient to capture certain bottom-up processes, such as bloom formation in response to nitrogen inputs or other physical dynamics such as stratification (Dahm et al., 2016; Dugdale et al., 2007; Lenocho et al., 2021). To better understand abiotic drivers of phytoplankton biomass in estuaries, measurements must more closely match the time-scales at which phytoplankton respond to their environment.

Of all the examined environmental drivers, water temperature had the strongest and most consistent associations with zooplankton biomass (Figure 4). However, as discussed in the previous section, water temperature was essentially a seasonal proxy—both copepods and cladoceran biomass displayed seasonality (Figure 2). Tidally-averaged discharge had negative effects on both taxa, consistent with observations of decreasing zooplankton biomass in more dynamic environments (Pace et al., 1992). Turbidity also negatively affected both zooplankton taxa, though effects were small and mechanisms behind this association are unclear. With the exception of water temperature, however, individual effects of environmental drivers were smaller than bottom-up effects of phytoplankton, especially in the landward reaches. Studies conducted in the SFE have previously demonstrated trophic interactions as more important controls on zooplankton biomass than abiotic factors (Kratina et al., 2014).

### Contribution of long-residence time habitats to estuarine food web productivity

Many estuaries have sustained severe losses of habitats such as tidal wetlands and terminal sloughs (Brophy et al., 2019; Whipple et al., 2012). These estuarine

habitats, characterized by high light availability and longer residence times, often support higher primary and secondary productivity than deeper or more turbulent areas (Ahearn et al., 2006; Bukaveckas et al., 2011), where phytoplankton are limited by access to the photic zone and both phytoplankton and zooplankton biomass is rapidly advected or dispersed (Breckenridge et al., 2020). Shallow, productive habitats can subsidize adjacent areas with lower in situ production (Lopez et al., 2006). Thus, loss of morphological and hydrodynamic heterogeneity in estuaries may have negative consequences for pelagic food webs. Though our study was conducted in a simplified, artificial channel, our results suggest that terminal estuarine habitats or other habitats with low exchange can support high zooplankton biomass. In impaired estuaries, both artificial and natural terminal habitats with long residence times may contribute high quality food resources to the pelagic food web (Frantzich et al., 2018), and help sustain imperiled populations of native fishes subject to food limitation (Hammock et al., 2021). Future work aimed at understanding the contribution of long-residence time habitats to pelagic food webs, or comparing trophic relationships across estuaries could prioritize (1) characterizing community composition in the context of hydrodynamic variation; (2) sampling with sufficient taxonomic resolution to quantify key trophic interactions and responses to abiotic drivers (Ward & Paerl, 2016), and (3) sampling phytoplankton at higher temporal frequency to match time-scales of responses to abiotic drivers such as nutrients.

### AUTHOR CONTRIBUTIONS

Erwin E. Van Nieuwenhuysse and Randy A. Dahlgren designed the study. Adrienne P. Smits designed and conducted the time series modeling, Matthew J. Young, Leah E. K. Lenocho, and Paul R. Stumpner contributed to data analysis. Adrienne P. Smits and Luke C. Loken made the figures. Adrienne P. Smits, Steven Sadro, Luke C. Loken, Matthew J. Young, Jon R. Burau, Paul R. Stumpner, Leah E. K. Lenocho, Erwin E. Van Nieuwenhuysse, and Tiffany Brown interpreted the data. Adrienne P. Smits lead manuscript writing, Steven Sadro, Luke C. Loken, Leah E. K. Lenocho, Paul R. Stumpner, Randy A. Dahlgren, and Matthew J. Young contributed to writing. All authors edited the manuscript.

### ACKNOWLEDGMENTS

Funding for this work was provided by US Bureau of Reclamation (agreements R18AC00040 and R20PG00028). Any use of trade, product or firm names is for descriptive purposes only and does not imply endorsement by the US Government. The views expressed are those of the authors and do not represent the views of the US Bureau of

Reclamation. The following USBR personnel assisted with field data collection: Nick Sakata, Harry Horner, Laura Benninger, Stuart Angerer, Melanie Lowe, Ian Smith, Andrew Richie and Brian Urbick. Phytoplankton and zooplankton enumeration were provided by BSA Environmental Services, Inc. Xien Wang analyzed water chemistry samples.

## CONFLICT OF INTEREST STATEMENT

The authors declare no conflict of interest.


## DATA AVAILABILITY STATEMENT


All data used in time series models (zooplankton and phytoplankton biomass, abiotic variables) are available from Smits et al. (2023) in the Environmental Data Initiative (EDI) Data Portal at <https://doi.org/10.6073/pasta/b763d8622a17123c5222c1a5179931f5>.

## ORCID

Adrienne P. Smits  <https://orcid.org/0000-0001-9967-5419>

Luke C. Loken  <https://orcid.org/0000-0003-3194-1498>

Matthew J. Young  <https://orcid.org/0000-0001-9306-6866>

Leah E. K. Lenoch  <https://orcid.org/0000-0003-4613-0858>

Steven Sadro  <https://orcid.org/0000-0002-6416-3840>

## REFERENCES

- Ahearn, D. S., J. H. Viers, J. F. Mount, and R. A. Dahlgren. 2006. "Priming the Productivity Pump: Flood Pulse Driven Trends in Suspended Algal Biomass Distribution Across a Restored Floodplain." *Freshwater Biology* 51(8): 1417–33. <https://doi.org/10.1111/j.1365-2427.2006.01580.x>.
- Alpine, A. E., and J. E. Cloern. 1988. "Phytoplankton Growth Rates in a Light-Limited Environment, San Francisco Bay." *Marine Ecology Progress Series* 44: 167–73.
- Armengol, L., G. Franchy, A. Ojeda, Á. Santana-del Pino, and S. Hernández-León. 2017. "Effects of Copepods on Natural Microplankton Communities: Do they Exert Top-Downcontrol?" *Marine Biology* 164(6): 1–13. <https://doi.org/10.1007/s00227-017-3165-2>.
- Bowen, A., G. Rollwagen-Bollens, S. M. Bollens, and J. Zimmerman. 2015. "Feeding of the Invasive Copepod *Pseudodiaptomus Forbesi* on Natural Microplankton Assemblages within the Lower Columbia River." *Journal of Plankton Research* 37(6): 1089–94. <https://doi.org/10.1093/plankt/fbv078>.
- Breckenridge, J., E. Pakhomov, S. Emry, and N. Mahara. 2020. "Copepod Assemblage Dynamics in a Snowmelt-Dominated Estuary." *Estuaries and Coasts* 43(6): 1502–18. <https://doi.org/10.1007/s12237-020-00722-3>.
- Breckenridge, J. K., S. M. Bollens, G. Rollwagen-Bollens, and G. C. Roegner. 2015. "Plankton Assemblage Variability in a River-Dominated Temperate Estuary during Late Spring (High-Flow) and Late Summer (Low-Flow) Periods." *Estuaries and Coasts* 38(1): 93–103. <https://doi.org/10.1007/s12237-014-9820-7>.
- Brett, M. T., and D. C. Müller-Navarra. 1997. "The Role of Highly Unsaturated Fatty Acids in Aquatic Foodweb Processes." *Freshwater Biology* 38(3): 483–99. <https://doi.org/10.1046/j.1365-2427.1997.00220.x>.
- Brophy, L. S., C. M. Greene, V. C. Hare, B. Holycross, A. Lanier, W. N. Heady, K. O'Connor, H. Imaki, T. Haddad, and R. Dana. 2019. "Insights into Estuary Habitat Loss in the Western United States Using a New Method for Mapping Maximum Extent of Tidal Wetlands." *PLoS One* 14(8): e0218558.
- Bukaveckas, P. A., L. E. Barry, M. J. Beckwith, V. David, and B. Lederer. 2011. "Factors Determining the Location of the Chlorophyll Maximum and the Fate of Algal Production within the Tidal Freshwater James River." *Estuaries and Coasts* 34(3): 569–82. <https://doi.org/10.1007/s12237-010-9372-4>.
- Bum, B. K., and F. R. Pick. 1996. "Factors Regulating Phytoplankton and Zooplankton Biomass in Temperate Rivers." *Limnology and Oceanography* 41(7): 1572–7. <https://doi.org/10.4319/lo.1996.41.7.1572>.
- Burnham, K. P., and D. R. Anderson. 2002. "Avoiding Pitfalls when Using Information-Theoretic Methods." *The Journal of Wildlife Management* 66(3): 912–8.
- Clesceri, L. S., A. E. Greenberg, and A. D. Eaton, eds. 1998. *Standard Methods for the Examination of Water and Wastewater*, 20th ed. Washington, DC: American Public Health Association, American Water Works Association, and Water Environment Association.
- Cloern, J. E., S. Q. Foster, and A. E. Kleckner. 2014. "Phytoplankton Primary Production in the world's Estuarine-Coastal Ecosystems." *Biogeosciences* 11(9): 2477–501. <https://doi.org/10.5194/bg-11-2477-2014>.
- Cloern, J. E. 1987. "Turbidity as a Control on Phytoplankton Biomass and Productivity in Estuaries." *Continental Shelf Research* 7(11–12): 1367–81. [https://doi.org/10.1016/0278-4343\(87\)90042-2](https://doi.org/10.1016/0278-4343(87)90042-2).
- Dahm, C. N., A. E. Parker, A. E. Adelson, M. A. Christman, and B. A. Bergamaschi. 2016. "Nutrient Dynamics of the Delta: Effects on Primary Producers." *San Francisco Estuary and Watershed Science* 14(4): 1–35. <https://doi.org/10.1544/sfews.2016v14iss4art4>.
- Deblois, C. P., A. Marchand, and P. Juneau. 2013. "Comparison of Photoacclimation in Twelve Freshwater Photoautotrophs (Chlorophyte, Bacillariophyte, Cryptophyte and Cyanophyte) Isolated from a Natural Community." *PLoS One* 8(3): e57139. <https://doi.org/10.1371/journal.pone.0057139>.
- Dexter, E., S. L. Katz, S. M. Bollens, G. Rollwagen-Bollens, and S. E. Hampton. 2020. "Modeling the Trophic Impacts of Invasive Zooplankton in a Highly Invaded River." *PLoS One* 15: 1–17. <https://doi.org/10.1371/journal.pone.0243002>.
- Dickman, E. M., J. M. Newell, M. J. González, and M. J. Vanni. 2008. "Light, Nutrients, and Food-Chain Length Constrain Planktonic Energy Transfer Efficiency across Multiple Trophic Levels." *Proceedings of the National Academy of Sciences* 105(47): 18408–12. <https://doi.org/10.1073/pnas.0805566105>.
- Doane, T. A., and W. R. Horwath. 2003. "Spectrophotometric Determination of Nitrate with a Single Reagent." *Analytical Letters* 36: 2713–22.
- Donázar-Aramendía, I., J. E. Sánchez-Moyano, I. García-Asencio, J. M. Miró, C. Megina, and J. C. García-Gómez. 2019. "Human

- Pressures on Two Estuaries of the Iberian Peninsula Are Reflected in Food Web Structure.” *Scientific Reports* 9(1): 1–10. <https://doi.org/10.1038/s41598-019-47793-2>.
- Downing, B. D., B. A. Bergamaschi, C. Kendall, T. E. C. Kraus, K. J. Dennis, J. A. Carter, and T. S. Von Dessonneck. 2016. “Using Continuous Underway Isotope Measurements to Map Water Residence Time in Hydrodynamically Complex Tidal Environments.” *Environmental Science and Technology* 50(24): 13387–96. <https://doi.org/10.1021/acs.est.6b05745>.
- Dugdale, R. C., F. P. Wilkerson, V. E. Hogue, and A. Marchi. 2007. “The Role of Ammonium and Nitrate in Spring Bloom Development in San Francisco Bay.” *Estuarine, Coastal and Shelf Science* 73(1–2): 17–29. <https://doi.org/10.1016/j.ecss.2006.12.008>.
- Dumont, H. J., I. Van de Velde, and S. Dumont. 1975. “The Dry Weight Estimate of Biomass in a Selection of Cladocera, Copepoda and Rotifera from the Plankton, Periphyton and Benthos of Continental Waters.” *Oecologia* 19: 75–97.
- Feyrer, F., S. B. Slater, D. E. Portz, D. Odom, T. Morgan-King, and L. R. Brown. 2017. “Pelagic Nekton Abundance and Distribution in the Northern Sacramento–San Joaquin Delta, California.” *Transactions of the American Fisheries Society* 146(1): 128–35. <https://doi.org/10.1080/00028487.2016.1243577>.
- Forster, J. C. 1995. “Soil Nitrogen.” In *Methods in Applied Soil Microbiology and Biochemistry*, edited by K. Alef and P. Nannipieri, 79–87. London: Academic Press.
- França, S., M. J. Costa, and H. N. Cabral. 2011. “Inter- and Intra-Estuarine Fish Assemblage Variability Patterns along the Portuguese Coast.” *Estuarine, Coastal and Shelf Science* 91(2): 262–71. <https://doi.org/10.1016/j.ecss.2010.10.035>.
- Frantzich, J., T. Sommer, and B. Schreier. 2018. “Physical and Biological Responses to Flow in a Tidal Freshwater Slough Complex.” *San Francisco Estuary and Watershed Science* 16(1): 1–26. <https://doi.org/10.15447/sfews.2018v16iss1/art3>.
- Galloway, A. W., and M. Winder. 2015. “Partitioning the Relative Importance of Phylogeny and Environmental Conditions on Phytoplankton Fatty Acids.” *PLoS One* 10(6): e0130053. <https://doi.org/10.1371/journal.pone.0130053>.
- Gameiro, C., P. Cartaxana, M. T. Cabrita, and V. Brotas. 2004. “Variability in Chlorophyll and Phytoplankton Composition in an Estuarine System.” *Hydrobiologia* 525(1): 113–24. <https://doi.org/10.1023/B:HYDR.0000038858.29164.31>.
- Ghosh, A., and P. Bhadury. 2019. “Exploring Biogeographic Patterns of Bacterioplankton Communities across Global Estuaries.” *MicrobiologyOpen* 8(5): e00741. <https://doi.org/10.1002/mbo3.741>.
- Gifford, S. M., G. Rollwagen-Bollens, and S. M. Bollens. 2007. “Mesozooplankton Omnivory in the Upper San Francisco Estuary.” *Marine Ecology Progress Series* 348: 33–46. <https://doi.org/10.3354/meps07003>.
- Glibert, P. M., R. C. Dugdale, F. Wilkerson, A. E. Parker, J. Alexander, E. Antell, S. Blaser, et al. 2014. “Major - but Rare - Spring Blooms in 2014 in San Francisco Bay Delta, California, a Result of the Long-Term Drought, Increased Residence Time, and Altered Nutrient Loads and Forms.” *Journal of Experimental Marine Biology and Ecology* 460: 8–18. <https://doi.org/10.1016/j.jembe.2014.06.001>.
- Glibert, P. M., F. P. Wilkerson, R. C. Dugdale, A. E. Parker, J. Alexander, S. Blaser, and S. Murasko. 2014. “Phytoplankton Communities from San Francisco Bay Delta Respond Differently to Oxidized and Reduced Nitrogen Substrates-Even under Conditions that Would Otherwise Suggest Nitrogen Sufficiency.” *Frontiers in Marine Science* 1(JUL): 1–16. <https://doi.org/10.3389/fmars.2014.00017>.
- Godin, G. 1972. *The Analysis of Tides*. Toronto, ON: University of Toronto Press.
- Griffiths, J. R., S. Hajdu, A. S. Downing, O. Hjerne, U. Larsson, and M. Winder. 2016. “Phytoplankton Community Interactions and Environmental Sensitivity in Coastal and Offshore Habitats.” *Oikos* 125(8): 1134–43. <https://doi.org/10.1111/oik.02405>.
- Guinder, V. A., J. C. Molinero, C. M. López Abbate, A. A. Berasategui, C. A. Popovich, C. V. Spetter, J. E. Marcovecchio, and R. H. Freije. 2017. “Phenological Changes of Blooming Diatoms Promoted by Compound Bottom-Up and Top-Down Controls.” *Estuaries and Coasts* 40(1): 95–104. <https://doi.org/10.1007/s12237-016-0134-9>.
- Hammock, B. G., R. Hartman, R. A. Dahlgren, C. Johnston, T. Kurobe, P. W. Lehman, L. S. Lewis, et al. 2021. “Patterns and Predictors of Condition Indices in a Critically Endangered Fish.” *Hydrobiologia* 849: 675–95. <https://doi.org/10.1007/s10750-021-04738-z>.
- Hampton, S. E., L. R. Izmest’eva, M. V. Moore, S. L. Katz, B. Dennis, and E. A. Silow. 2008. “Sixty Years of Environmental Change in the world’s Largest Freshwater Lake–Lake Baikal, Siberia.” *Global Change Biology* 14(8): 1947–58. <https://doi.org/10.1111/j.1365-2486.2008.01616.x>.
- Hampton, S. E., M. D. Scheuerell, M. J. Church, and J. M. Melack. 2019. “Long-Term Perspectives in Aquatic Research.” *Limnology and Oceanography* 64(Moss 2012): S2–S10. <https://doi.org/10.1002/lno.11092>.
- Hampton, S. E., M. D. Scheuerell, and D. E. Schindler. 2006. “Coalescence in the Lake Washington Story: Interaction Strengths in a Planktonic Food Web.” *Limnology and Oceanography* 51(5): 2042–51. <https://doi.org/10.4319/lo.2006.51.5.2042>.
- Harding, L. W., C. L. Gallegos, E. S. Perry, W. D. Miller, J. E. Adolf, M. E. Mallonee, and H. W. Paerl. 2016. “Long-Term Trends of Nutrients and Phytoplankton in Chesapeake Bay.” *Estuaries and Coasts* 39(3): 664–81. <https://doi.org/10.1007/s12237-015-0023-7>.
- Hillebrand, H., C. D. Dürselen, D. Kirschtel, U. Pollinger, and T. Zohary. 1999. “Biovolume Calculation for Pelagic and Benthic Microalgae.” *Journal of Phycology* 35: 403–24.
- Hoellein, T. J., D. A. Bruesewitz, and D. C. Richardson. 2013. “Revisiting Odum (1956): A Synthesis of Aquatic Ecosystem Metabolism.” *Limnology and Oceanography* 58(6): 2089–100. <https://doi.org/10.4319/lo.2013.58.6.2089>.
- Holmes, E. E., E. J. Ward, and M. D. Scheuerell. 2018. *Analysis of Multivariate Time-Series Using the MARSS Package*. Seattle, WA: DOC-NOAA-NMFS-NWC.
- Holmes, E. E., E. J. Ward, and K. Wills. 2012. “MARSS: Multivariate Autoregressive State-Space Models for Analyzing Time-Series Data.” *R Journal* 4(1): 11–9. <https://doi.org/10.32614/rj-2012-002>.
- Howarth, R., F. Chan, D. J. Conley, J. Garnier, S. C. Doney, R. Marino, and G. Billen. 2011. “Coupled Biogeochemical Cycles: Eutrophication and Hypoxia in Temperate Estuaries

- and Coastal Marine Ecosystems.” *Frontiers in Ecology and the Environment* 9(1): 18–26. <https://doi.org/10.1890/100008>.
- Howarth, R. W., D. P. Swaney, T. J. Butler, and R. Marino. 2000. “Climatic Control on Eutrophication of the Hudson River Estuary.” *Ecosystems* 3(2): 210–5. <https://doi.org/10.1007/s100210000020>.
- Irigoin, X., R. P. Harris, H. M. Verheye, P. Joly, J. Runge, M. Starr, D. Pond, et al. 2002. “Copepod Hatching Success in Marine Ecosystems with High Diatom Concentrations.” *Nature* 419(6905): 387–9. <https://doi.org/10.1038/nature01055>.
- Ives, A. R., B. Dennis, K. L. Cottingham, and S. R. Carpenter. 2003. “Estimating Community Stability and Ecological Interactions from Time-Series Data.” *Ecological Monographs* 73(2): 301–30. [https://doi.org/10.1890/0012-9615\(2003\)073\[0301:ECSAEI\]2.0.CO;2](https://doi.org/10.1890/0012-9615(2003)073[0301:ECSAEI]2.0.CO;2).
- Jankowski, K. J., J. N. Houser, M. D. Scheuerell, and A. P. Smits. 2021. “Warmer Winters Increase the Biomass of Phytoplankton in a Large Floodplain River.” *Journal of Geophysical Research: Biogeosciences* 126(9): e2020JG006135. <https://doi.org/10.1029/2020JG006135>.
- Jassby, A. D., J. E. Cloern, and B. E. Cole. 2002. “Annual Primary Production: Patterns and Mechanisms of Change in a Nutrient-Rich Tidal Ecosystem.” *Limnology and Oceanography* 47(3): 698–712. <https://doi.org/10.4319/lo.2002.47.3.0698>.
- Jungbluth, M., C. Lee, C. Patel, T. Ignoffo, B. Bergamaschi, and W. Kimmerer. 2021. “Production of the Copepod Pseudodiaptomus Forbesi Is Not Enhanced by Ingestion of the Diatom Aulacoseira Granulata during a Bloom.” *Estuaries and Coasts* 44(4): 1083–99. <https://doi.org/10.1007/s12237-020-00843-9>.
- Kayfetz, K., S. M. Bashevkin, M. Thomas, R. Hartmann, C. E. Burdi, A. Hennessy, T. Tempel, and A. Barros. 2020. *Zooplankton Integrated Dataset Metadata Report. IEP Technical Report 93*. Sacramento, CA: California Department of Water Resources.
- Kennish, M. J. 2002. “Environmental Threats and Environmental Future of Estuaries.” *Environmental Conservation* 29(1): 78–107. <https://doi.org/10.1017/S0376892902000061>.
- Kimmerer, W., T. R. Ignoffo, B. Bemowski, J. Modéran, A. Holmes, and B. Bergamaschi. 2018. “Zooplankton Dynamics in the Cache Slough Complex of the Upper San Francisco Estuary.” *San Francisco Estuary and Watershed Science* 16(3): 1–25. <https://doi.org/10.15447/sfews.2018v16iss3art4>.
- Kimmerer, W. J., A. E. Parker, U. E. Lidström, and E. J. Carpenter. 2012. “Short-Term and Interannual Variability in Primary Production in the Low-Salinity Zone of the San Francisco Estuary.” *Estuaries and Coasts* 35(4): 913–29. <https://doi.org/10.1007/s12237-012-9482-2>.
- Kimmerer, W. J., and J. K. Thompson. 2014. “Phytoplankton Growth Balanced by Clam and Zooplankton Grazing and Net Transport into the Low-salinity Zone of the San Francisco Estuary.” *Estuaries and Coasts* 37: 1202–18. <https://doi.org/10.1007/s12237-013-9753-6>.
- Kratina, P., R. Mac Nally, W. J. Kimmerer, J. R. Thomson, and M. Winder. 2014. “Human-Induced Biotic Invasions and Changes in Plankton Interaction Networks.” *Journal of Applied Ecology* 51(4): 1066–74. <https://doi.org/10.1111/1365-2664.12266>.
- Lapierre, J. F., and J. J. Frenette. 2008. “Advection of Freshwater Phytoplankton in the St. Lawrence River Estuarine Turbidity Maximum as Revealed by Sulfur-Stable Isotopes.” *Marine Ecology Progress Series* 372: 19–29. <https://doi.org/10.3354/meps07685>.
- Lawrence, S. G., D. F. Malley, W. J. Findlay, M. A. MacIver, and I. L. Delbaere. 1987. “Method for Estimating Dry Weight of Freshwater Planktonic Crustaceans from Measures of Length and Shape.” *Canadian Journal of Fisheries and Aquatic Sciences* 44: 264–74.
- Lee, D. Y., D. P. Keller, B. C. Crump, and R. R. Hood. 2012. “Community Metabolism and Energy Transfer in the Chesapeake Bay Estuarine Turbidity Maximum.” *Marine Ecology Progress Series* 449: 65–82. <https://doi.org/10.3354/meps09543>.
- Lehman, P. W. 2000. “The Influence of Climate on Phytoplankton Community Biomass in San Francisco Bay Estuary.” *Limnology and Oceanography* 45(3): 580–90. <https://doi.org/10.4319/lo.2000.45.3.0580>.
- Lenoch, L. E. K., P. R. Stumpner, J. R. Burau, L. C. Loken, and S. Sadro. 2021. “Dispersion and Stratification Dynamics in the Upper Sacramento Deep Water Ship Channel.” *San Francisco Estuary and Watershed Science* 19(4): 1–29. <https://doi.org/10.15447/sfews.2021v19iss4art5>.
- Lionard, M., F. Azémar, S. Boulétreau, K. Muylaert, M. Tackx, and W. Vyverman. 2005. “Grazing by Meso- and Microzooplankton on Phytoplankton in the Upper Reaches of the Schelde Estuary (Belgium/The Netherlands).” *Estuarine, Coastal and Shelf Science* 64(4): 764–74. <https://doi.org/10.1016/j.ecss.2005.04.011>.
- Loken, L. C., S. Sadro, L. E. K. Lench, P. R. Stumpner, R. A. Dahlgren, J. R. Burau, and E. E. Van Nieuwenhuysse. 2022. “Whole Ecosystem Experiment Illustrates Short Time-Scale Hydrodynamic, Light, and Nutrient Control of Primary Production in a Terminal Slough.” *Estuaries and Coasts* 45: 2428–49. <https://doi.org/10.1007/s12237-022-01111-8>.
- Lopez, C. B., J. E. Cloern, T. S. Schraga, A. J. Little, L. V. Lucas, J. K. Thompson, and J. R. Burau. 2006. “Ecological Values of Shallow-Water Habitats: Implications for the Restoration of Disturbed Ecosystems.” *Ecosystems* 9(3): 422–40. <https://doi.org/10.1007/s10021-005-0113-7>.
- Lotze, H. K., H. S. Lenihan, B. J. Bourque, R. H. Bradbury, R. G. Cooke, M. C. Kay, S. M. Kidwell, M. X. Kirby, C. H. Peterson, and J. B. C. Jackson. 2006. “Depletion, Degradation, and Recover Potential of Estuaries and Coastal Seas.” *Science* 312: 1806–9.
- Lotze, H. K., and I. Milewski. 2004. “Two Centuries of Multiple Human Impacts and Successive Changes in a North Atlantic Food Web.” *Ecological Applications* 14(5): 1428–47.
- Lucas, L. V., D. M. Sereno, J. R. Burau, T. S. Schraga, C. B. Lopez, M. T. Stacey, K. V. Parchevsky, and V. P. Parchevsky. 2006. “Intradaily Variability of Water Quality in a Shallow Tidal Lagoon: Mechanisms and Implications.” *Estuaries and Coasts* 29(5): 711–30. <https://doi.org/10.1007/BF02786523>.
- Lucas, L. V., and J. K. Thompson. 2012. “Changing Restoration Rules: Exotic Bivalves Interact with Residence Time and Depth to Control Phytoplankton Productivity.” *Ecosphere* 3(12): 1–26. <https://doi.org/10.1890/ES12-00251.1>.
- Lucas, L. V., J. K. Thompson, and L. R. Brown. 2009. “Why Are Diverse Relationships Observed between Phytoplankton Biomass and Transport Time?” *Limnology and Oceanography* 54(1): 381–90. <https://doi.org/10.4319/lo.2009.54.1.0381>.

- Manier, J. T., R. J. Haro, J. N. Houser, and E. A. Strauss. 2021. "Spatial and Temporal Dynamics of Phytoplankton Assemblages in the Upper Mississippi River." *River Research and Applications* 37(10): 1451–62. <https://doi.org/10.1002/rra.3852>.
- McCauley, E. 1984. "The Estimation of the Abundance and Biomass of Zooplankton in Samples." In *A Manual for the Assessment of Secondary Productivity in Fresh Waters*, edited by J. A. Downing and F. H. Rigler, 228–65. Oxford, UK: Blackwell Scientific Publishers.
- McClelland, J. W., and I. Valiela. 1998. "Changes in Food Web Structure under the Influence of Increased Anthropogenic Nitrogen Inputs to Estuaries." *Marine Ecology Progress Series* 168: 259–71. <https://doi.org/10.3354/meps168259>.
- McNabb, C. D. 1960. "Enumeration of Freshwater Phytoplankton Concentrated on the Membrane Filter." *Limnology and Oceanography* 5: 57–61.
- Monsen, N. E., J. E. Cloern, L. V. Lucas, and S. G. Monismith. 2002. "A Comment on the Use of Flushing Time, Residence Time, and Age as Transport Time Scales." *Limnology and Oceanography* 47(5): 1545–53. <https://doi.org/10.4319/lo.2002.47.5.1545>.
- Montgomery, J. R., P. B. Moyle, and R. A. Dahlgren. 2017. "Foodweb Dynamics in Shallow Tidal Sloughs of the San Francisco Estuary." Master's thesis, University of California Davis.
- Pace, M. L., S. E. G. Findlay, and D. Lints. 1992. "Zooplankton in Advective Environments: The Hudson River Community and a Comparative Analysis." *Canadian Journal of Fisheries and Aquatic Sciences* 49(5): 1060–9. <https://doi.org/10.1139/f92-117>.
- Paerl, H. W., K. L. Rossignol, S. N. Hall, B. L. Peierls, and M. S. Wetz. 2010. "Phytoplankton Community Indicators of Short- and Long-Term Ecological Change in the Anthropogenically and Climatically Impacted Neuse River Estuary, North Carolina, USA." *Estuaries and Coasts* 33(2): 485–97. <https://doi.org/10.1007/s12237-009-9137-0>.
- Park, G. S., and H. G. Marshall. 2000. "The Trophic Contributions of Rotifers in Tidal Freshwater and Estuarine Habitats." *Estuarine, Coastal and Shelf Science* 51(6): 729–42. <https://doi.org/10.1006/ecss.2000.0723> Get rights and content.
- Parker, A. E., W. J. Kimmerer, and U. U. Lidström. 2012. "Reevaluating the Generality of an Empirical Model for Light-Limited Primary Production in the San Francisco Estuary." *Estuaries and Coasts* 35(4): 930–42. <https://doi.org/10.1007/s12237-012-9507-x>.
- Pennock, J. R., and J. H. Sharp. 1986. "Phytoplankton Production in the Delaware Estuary: Temporal and Spatial Variability." *Marine Ecology Progress Series* 34(1/2): 143–55.
- Pihl, L., A. Cattrijsse, I. Codling, S. Mathieson, D. S. McLusky, and C. Roberts. 2002. "Habitat Use by Fishes in Estuaries and Other Brackish Areas." In *Fishes in Estuaries*, edited by M. Elliot and K. Hemingway, 10–53. Oxford, UK: Blackwell Scientific Publishers.
- R Core Team. 2020. *R: A Language and Environment for Statistical Computing*. Vienna: R Foundation for Statistical Computing.
- Reynolds, C. S., and J. P. Descy. 1996. "The Production, Biomass and Structure of Phytoplankton in Large Rivers." *Large Rivers* 10: 161–87. <https://doi.org/10.1127/lr/10/1996/161>.
- Sartory, D. P., and J. U. Grobbelaar. 1984. "Extraction of Chlorophyll-a from Freshwater Phytoplankton for Spectrophotometric Analysis." *Hydrobiologia* 114: 177–87.
- Schuchardt, B., and M. Schirmer. 1991. "Phytoplankton Maxima in the Tidal Freshwater Reaches of Two Coastal Plain Estuaries." *Estuarine, Coastal and Shelf Science* 32(2): 187–206. [https://doi.org/10.1016/0272-7714\(91\)90014-3](https://doi.org/10.1016/0272-7714(91)90014-3).
- Smits, A. P., E. VanNieuwenhuysse, R. Dahlgren, and P. Stumpner. 2023. "Water Quality, Phytoplankton, and Zooplankton in the Sacramento Deep Water Ship Channel, CA ver 1." Environmental Data Initiative. <https://doi.org/10.6073/pasta/b763d8622a17123c5222c1a5179931f5>.
- Sommer, T., C. Armor, R. Baxter, R. Breuer, L. Brown, M. Chotkowski, S. Culbertson, et al. 2007. "The Collapse of Pelagic Fishes in the Upper San Francisco Estuary." *Fisheries* 32(6): 270–7.
- Sommer, T., and F. Mejia. 2013. "A Place to Call Home: A Synthesis of Delta Smelt Habitat in the Upper San Francisco Estuary." *San Francisco Estuary and Watershed Science* 11(2): 1–25. <https://doi.org/10.15447/sfews.2013v11iss2art4>.
- Sommer, U., and F. Sommer. 2006. "Cladocerans versus Copepods: The Cause of Contrasting Top-Down Controls on Freshwater and Marine Phytoplankton." *Oecologia* 147: 183–94. <https://doi.org/10.1007/s00442-005-0320-0>.
- Stibor, H., O. Vadstein, S. Diehl, A. Gelzleichter, T. Hansen, F. Hantzsche, A. Katechakis, et al. 2004. "Copepods Act as a Switch between Alternative Trophic Cascades in Marine Pelagic Food Webs." *Ecology Letters* 7: 321–8. <https://doi.org/10.1111/j.1461-0248.2004.00580.x>.
- Stumpner, E. B., B. A. Bergamaschi, T. E. C. Kraus, A. E. Parker, F. P. Wilkerson, B. D. Downing, R. C. Dugdale, et al. 2020. "Spatial Variability of Phytoplankton in a Shallow Tidal Freshwater System Reveals Complex Controls on Abundance and Community Structure." *Science of the Total Environment* 700: 134392. <https://doi.org/10.1016/j.scitotenv.2019.134392>.
- Stumpner, P. R., J. R. Burau, and A. L. Forrest. 2020. "A Lagrangian-to-Eulerian Metric to Identify Estuarine Pelagic Habitats." *Estuaries and Coasts* 44(5): 1231–49. <https://doi.org/10.1007/s12237-020-00861-7>.
- Suzuki, K. W., K. Nakayama, and M. Tanaka. 2013. "Distinctive Copepod Community of the Estuarine Turbidity Maximum: Comparative Observations in Three Macrotidal Estuaries (Chikugo, Midori, and Kuma Rivers), Southwestern Japan." *Journal of Oceanography* 69(1): 15–33. <https://doi.org/10.1007/s10872-012-0151-7>.
- Tan, Y., L. Huang, Q. Chen, and X. Huang. 2004. "Seasonal Variation in Zooplankton Composition and Grazing Impact on Phytoplankton Standing Stock in the Pearl River Estuary, China." *Continental Shelf Research* 24(16): 1949–68. <https://doi.org/10.1016/j.csr.2004.06.018>.
- Thompson, P. A., P. I. Bonham, and K. M. Swadling. 2008. "Phytoplankton Blooms in the Huon Estuary, Tasmania: Top-Down or Bottom-Up Control?" *Journal of Plankton Research* 30(7): 735–53. <https://doi.org/10.1093/plankt/fbn044>.
- United States Geological Survey. 2021. "USGS Water Data for the Nation: U.S. Geological Survey National Water Information System database." <https://doi.org/10.5066/F7P55KJN>.
- Valdes-Weaver, L. M., M. F. Piehler, J. L. Pinckney, K. E. Howe, K. Rossignol, and H. W. Paerl. 2006. "Long-Term Temporal and Spatial Trends in Phytoplankton Biomass and Class-Level Taxonomic Composition in the Hydrologically Variable Neuse-Pamlico Estuarine Continuum, North Carolina, U.S.A." *Limnology and Oceanography* 51(3): 1410–20. <https://doi.org/10.4319/lo.2006.51.3.1410>.

- Vinagre, C., and M. J. Costa. 2014. "Estuarine-Coastal Gradient in Food Web Network Structure and Properties." *Marine Ecology Progress Series* 503: 11–21. <https://doi.org/10.3354/meps10722>.
- Walsh, J. R., R. C. Lathrop, and M. J. Vander Zanden. 2018. "Uncoupling Indicators of Water Quality Due to the Invasive Zooplankter, *Bythotrephes longimanus*." *Limnology and Oceanography* 63(3): 1313–27. <https://doi.org/10.1002/lno.10773>.
- Ward, A., and H. W. Paerl. 2016. "Role of Nutrients in Shifts in Phytoplankton Abundance and Species Composition in the Sacramento-San Joaquin Delta." In *Delta Nutrient Forms and Ratios Public Workshop* 1–41. Sacramento. [https://www.waterboards.ca.gov/centralvalley/water\\_issues/delta\\_water\\_quality/delta\\_nutrient\\_research\\_plan/science\\_work\\_groups/2017\\_0530\\_phyto\\_wp.pdf](https://www.waterboards.ca.gov/centralvalley/water_issues/delta_water_quality/delta_nutrient_research_plan/science_work_groups/2017_0530_phyto_wp.pdf).
- Wetz, M. S., H. W. Paerl, J. C. Taylor, and J. A. Leonard. 2011. "Environmental Controls upon Picophytoplankton Growth and Biomass in a Eutrophic Estuary." *Aquatic Microbial Ecology* 63(2): 133–43. <https://doi.org/10.3354/ame01488>.
- Whipple, A. A., R. M. Grossinger, D. Rankin, B. Stanford, and R. A. Askevold. 2012. "Sacramento–San Joaquin Delta Historical Ecology Investigation: Exploring Pattern and Process." In *SFEI Contribution No. 672*. Richmond, CA: SFEI.
- Winder, M., J. Carstensen, A. W. E. Galloway, H. H. Jakobsen, and J. E. Cloern. 2017. "The Land-Sea Interface: A Source of High-Quality Phytoplankton to Support Secondary Production." *Limnology and Oceanography* 62: S258–71. <https://doi.org/10.1002/lno.10650>.
- Winder, M., and A. D. Jassby. 2011. "Shifts in Zooplankton Community Structure: Implications for Food Web Processes in the Upper San Francisco Estuary." *Estuaries and Coasts* 34(4): 675–90. <https://doi.org/10.1007/s12237-010-9342-x>.
- Wood, S. 2022. "mgcv: Mixed GAM Computation Vehicle with Automatic Smoothness Estimation." R package version 1.8-40; [accessed 2022 August 25]. Available from <http://cran.r-project.org/web/packages/mgcv>.
- York, J. K., G. B. McManus, W. J. Kimmerer, A. M. Slaughter, and T. R. Ignoffo. 2014. "Trophic Links in the Plankton in the Low Salinity Zone of a Large Temperate Estuary: Top-Down Effects of Introduced Copepods." *Estuaries and Coasts* 37(3): 576–88. <https://doi.org/10.1007/s12237-013-9698-9>.
- Young, M. J., F. Feyrer, P. R. Stumpner, V. Larwood, O. Patton, and L. R. Brown. 2021. "Hydrodynamics Drive Pelagic Communities and Food Web Structure in a Tidal Environment." *International Review of Hydrobiology* 106(2): 69–85. <https://doi.org/10.1002/iroh.202002063>.
- Young, M. J., E. Howe, T. O'Rear, K. Berridge, and P. Moyle. 2021. "Food Web Fuel Differs across Habitats and Seasons of a Tidal Freshwater Estuary." *Estuaries and Coasts* 44(1): 286–301. <https://doi.org/10.1007/s12237-020-00762-9>.

## SUPPORTING INFORMATION

Additional supporting information can be found online in the Supporting Information section at the end of this article.

**How to cite this article:** Smits, Adrienne P., Luke C. Loken, Erwin E. Van Nieuwenhuysse, Matthew J. Young, Paul R. Stumpner, Leah E. K. Lenocho, Jon R. Burau, Randy A. Dahlgren, Tiffany Brown, and Steven Sadro. 2023. "Hydrodynamics Structure Plankton Communities and Interactions in a Freshwater Tidal Estuary." *Ecological Monographs* 93(2): e1567. <https://doi.org/10.1002/ecm.1567>